THE JOURNAL OF BIOLOGICAL CHEMISTRY VOL. 280, NO. 52, pp. 42826–42830, December 30, 2005

Transgenic Small Interfering RNA Halts Amyotrophic Lateral Sclerosis in a Mouse Model*[S]

Received for publication, July 15, 2005, and in revised form, September 23, 2005 Published, JBC Papers in Press, October 12, 2005, DOI 10.1074/jbc.M507685200

Yuki Saito[‡1], Takanori Yokota[‡1,2], Tasuku Mitani[§], Kaoru Ito[‡], Masayuki Anzai[§], Makoto Miyagishi[¶], Kazunari Taira[¶], and Hidehiro Mizusawa[‡‖]

From the [‡]Department of Neurology and Neurological Science, Graduate School, Tokyo Medical and Dental University, 1-5-45 Yushima, Bunkyo-ku, Tokyo 113-8519, the [§]Institute of Advanced Technology, Kinki University, 14-1 Minami-Akasaka, Kainan, Wakayama 642-0017, the [¶]Department of Chemistry and Biotechnology, School of Engineering, The University of Tokyo, 7-3-1 Hongo, Bunkyo-ku, Tokyo 113-0013, and the [‖]21st Century COE Program on Brain Integration and Its Disorders, Tokyo Medical and Dental University, 1-5-45 Yushima, Bunkyo-ku, Tokyo 113-8519, Japan

Many autosomal dominant diseases such as familial amyotrophic lateral sclerosis (ALS) with copper/zinc superoxide dismutase (SOD1) mutation may be induced by missense point mutations that result in the production of proteins with toxic properties. Reduction in the encoding of proteins from such mutated genes can therefore be expected to improve the disease phenotype. The duplex of 21-nucleotide RNA, known as small interfering RNA (siRNA), has recently emerged as a powerful gene silencing tool. We made transgenic (Tg) mice with modified siRNA, which had multiple mismatch alternations within the sense strand, to prevent the "shutdown phenomenon" of transgenic siRNA. Consequently, the *in vivo* knockdown effect of siRNA on SOD1 expression did not diminish over four generations. When we crossed these anti-SOD1 siRNA Tg mice with $SOD1^{G93A}$ Tg mice, a model for ALS, siRNA prevented the development of disease by inhibiting mutant G93A SOD1 production in the central nervous system. Our findings clearly proved the principle that siRNA-mediated gene silencing can stop the development of familial ALS with SOD1 mutation.

RNA interference is the process of sequence-specific, post-transcriptional gene silencing, initiated by double-stranded RNA. RNA interference is a multistep process that involves generation of 21–23-nucleotide small interfering RNA (siRNA),[3] resulting in degradation of homologous RNA. One rational approach to therapy using siRNA is to eliminate the aberrant protein encoded by mutant alleles in dominantly inherited diseases.

Amyotrophic lateral sclerosis (ALS) is a fatal neurodegenerative disease characterized by the degeneration of motor neurons in the central nervous system. Although most cases of ALS are sporadic, 5–10% of ALS cases are familial, and of these, ~20% are due to missense point mutations in the gene encoding copper/zinc superoxide dismutase (SOD1) (1). Recent studies using transgenic (Tg) mice and cell culture models of ALS with SOD1 mutations have indicated that SOD1 mutations induce the disease by their toxic properties, not by a loss of SOD1 activity (2). Therefore, inhibition of mutated allele expression is expected to provide a direct approach to therapy for this type of familial ALS. In cultured cells, siRNA can effectively inhibit the production of mutant proteins in various neurodegenerative diseases including ALS (3). Furthermore, virus-mediated siRNA delivered by direct injection of viral vectors to the brain or muscle delays phenotypic expression in Tg mice *in vivo* (4–7). However, it has not been proved in principle whether inhibition of mutant genes with siRNA can truly stop dominantly inherited diseases. The most difficult problem in *in vivo* therapy with siRNA is that there is no sophisticated method of delivering siRNA throughout the central nervous system. Therefore, to answer this question, as a first step, we tried to make siRNA Tg mice in which siRNA was ubiquitously expressed in the brain, and we then crossed these siRNA Tg mice with $SOD1^{G93A}$ Tg mice to efficiently deliver siRNA throughout the central nervous system.

Moreover, we utilized modified short hairpin RNA (shRNA), which has mismatch alternations within the sense strand, to make Tg mice. This method was able to enhance the genetic stability of the shRNA expression cassette in the genome over generations.

MATERIALS AND METHODS

Construction of Anti-SOD1 shRNA Expression Vector—We generated an anti-SOD1 shRNA cassette as reported previously (3). We inserted the anti-SOD1 shRNA cassette immediately downstream of the human U6 promoter in pUC19 (Takara, Tokyo, Japan), with a PGK-neo-poly(A) cassette (Fig. 1*A*). Three G → A alternations were introduced (denoted by asterisks below) in the sense strand: 5′-GGUGG*AAAUG*AAGAAAG*UAC-3′ (Fig. 1*B*). This sequence was a good and common siRNA target region in both human and mouse SOD1 mRNAs. To select this target site, we performed a BLAST similarity search to minimize off-target effects.

Generation of Anti-SOD1 siRNA Tg Mice—To produce anti-SOD1 siRNA Tg mice, the anti-SOD1 shRNA expression vector was introduced into 129/Sv embryonic stem (ES) cells (Chemicon, Temecula, CA) by electroporation, and individual stable integrants were tested for expression of SOD1 protein by Western blot analysis. ES cell clones that exhibited greatly decreased SOD1 expression were injected into C57BL/6 blastocysts (CLEA Japan, Tokyo, Japan), and the resulting chimeric male mice were mated with C57BL/6 females. The offspring, in which germline transmission was determined by the following PCR method, were referred to as anti-SOD1 siRNA Tg mice.

Double Tg mice were generated by crossing $SOD1^{G93A}$ Tg mice (G1H line from Jackson Laboratories, backcrossed to C57BL/6 mice) with anti-SOD1 siRNA Tg mice. Genotypes of these mice were determined

* This study was supported by grants from the Ministry of Education, Science and Culture, Japan (to T. Y.) and the Ministry of Health, Labor and Welfare, Japan (to T. Y. and H. M.). The costs of publication of this article were defrayed in part by the payment of page charges. This article must therefore be hereby marked "*advertisement*" in accordance with 18 U.S.C. Section 1734 solely to indicate this fact.

[S] The on-line version of this article (available at http://www.jbc.org) contains a supplemental movie and a supplemental figure.

[1] Both authors contributed equally to this work.

[2] To whom correspondence should be addressed. Tel.: 81-3-5803-5234; Fax: 81-3-5803-0169; E-mail: tak-yokota.nuro@tmd.ac.jp.

[3] The abbreviations used are: siRNA, small interfering RNA; shRNA, short hairpin RNA; ALS, amyotrophic lateral sclerosis; SOD1, copper/zinc superoxide dismutase; Tg, transgenic; ES, embryonic stem.

by PCR analysis of tail DNA. PCR was carried out using the following primer sets: 5′-CTTGGGTAGTTTGCAG-3′ and 5′-CAGGAAACAGCTATGAC-3′ for anti-SOD1 siRNA Tg mice and 5′-CATCAGCCCTAATCCATCTGA-3′ and 5′-CGCGACTAACAATCAAAGTGA-3′ for $SOD1^{G93A}$ Tg mice. The mice were maintained under pathogen-free conditions and handled in accordance with the Guidelines for Animal Experimentation of the Institute for Advanced Technology of Kinki University and of Tokyo Medical and Dental University.

Northern Blot Analysis—Mice were deeply anesthetized with pentobarbital sodium, sacrificed, and perfused with cold phosphate-buffered saline. Total RNA was extracted from the brain and spinal cord by using TRIzol (Invitrogen). Total RNA (20 μg) was fractionated on a 1% formaldehyde agarose gel and transferred to a Nytran membrane (Schleicher & Schuell). The lower part of the membrane was hybridized with a purified PCR fragment, corresponding to mouse SOD1 cDNA (bases 15–495); it was labeled with fluorescein by using a Gene Images random-prime labeling kit (Amersham Biosciences). The upper part of the membrane was hybridized with a probe specific for β-actin. The signals were visualized with a Gene Images CDP-star detection kit (Amersham Biosciences). For detection of small RNA, total RNA (25 μg) was separated by electrophoresis on a 14% polyacrylamide-urea gel and transferred to a Hybond-N+ membrane (Amersham Biosciences). The blot was hybridized with a probe of the non-mutated sense sequence of shRNA, which was labeled with fluorescein by using a Gene Images 3′-Oligolabeling kit (Amersham Biosciences) and visualized as mentioned above.

Western Blot Analysis—ES cell lysates were prepared with radioimmune precipitation buffer (150 mM NaCl, 1% Nonidet P-40, 0.5% sodium deoxycholate, 0.1% SDS). Protein samples were extracted from tails, brains, and spinal cords and homogenized in buffer containing 0.1% SDS, 1% Triton X-100, 1% sodium deoxycholate, and 1 mM phenylmethylsulfonyl fluoride. Equal amounts of extracted protein were mixed with Laemmli sample buffer, denatured, and separated on 15% SDS-PAGE. After transfer to a polyvinylidene difluoride membrane (Bio-Rad), blots were probed with anti-SOD1 polyclonal antibody S-100 (1:7000, StressGen Biotechnologies, Victoria, British Columbia, Canada) or anti-β-tubulin monoclonal antibody (1:500, BD Biosciences) followed by the relevant horseradish peroxidase-conjugated immunoglobulin (Amersham Biosciences). Immunoblots were detected using ECL reagent (Amersham Biosciences).

Immunohistochemical and Histopathological Analyses—The lumbar segments of the spinal cords were removed and fixed in 4% paraformaldehyde in phosphate-buffered saline, pH 7.4. They were cryoprotected with sucrose solution and frozen in Tissue-Tek O.C.T. compound (Sakura Finetechnical Co., Tokyo, Japan). For immunohistochemistry, sections (10 μm thick) of the spinal cord at the level of the third lumbar (L3) vertebra from anti-SOD1 siRNA Tg mice and wild-type littermates were mounted onto the same gelatin-coated slide and incubated with anti-SOD1 polyclonal

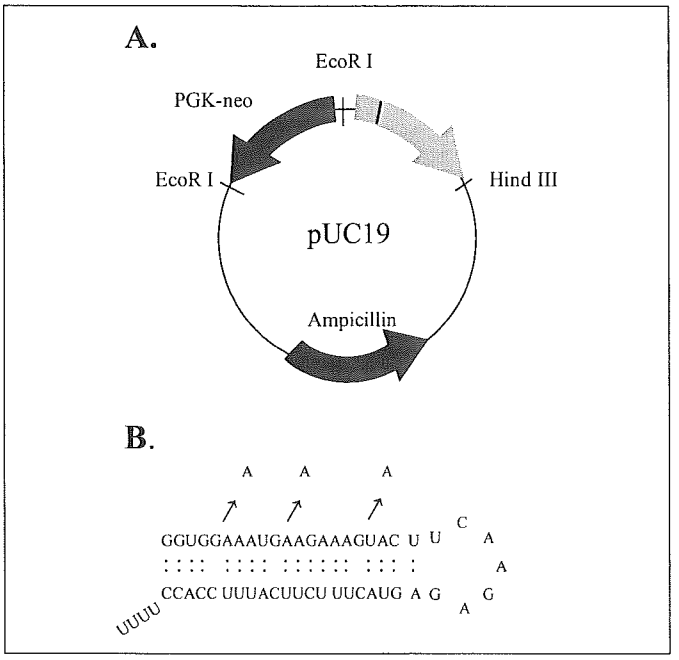

FIGURE 1. **Construction of anti-SOD1 shRNA expression vector.** *A*, the anti-SOD1 shRNA expression vector included an anti-SOD1 shRNA cassette with human U6 promoter and a PGK-neo-poly(A) cassette. *B*, predicted secondary structure of anti-SOD1 shRNA. Three G → A alternations were introduced, but only in the sense sequence of shRNA (*arrows*).

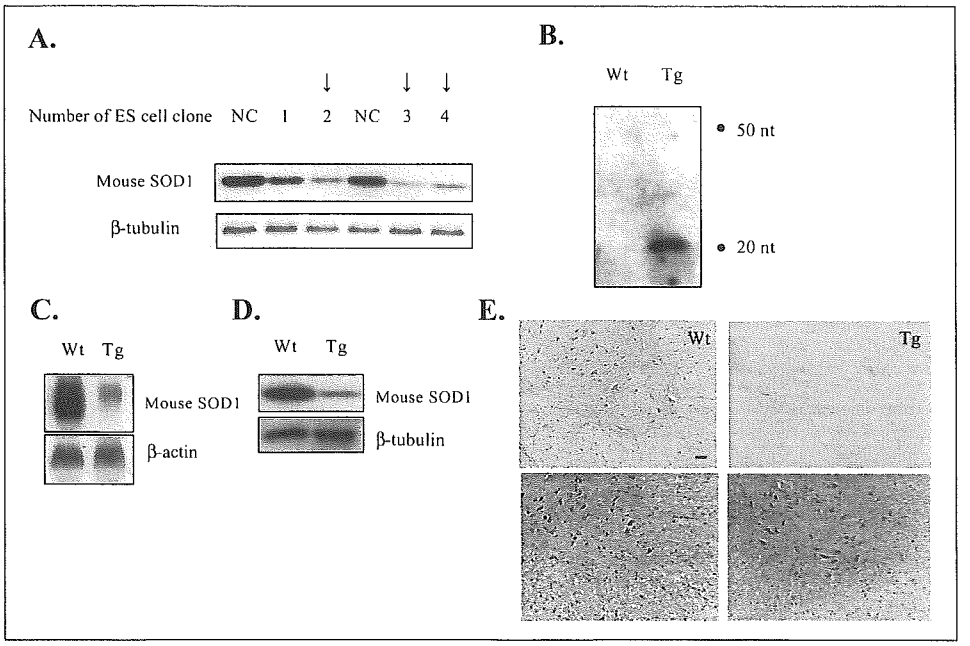

FIGURE 2. **Efficient knockdown of SOD1 in anti-SOD1 siRNA Tg mice.** *A*, production of SOD1 protein in four different ES cell clones on Western blot analysis. *NC* = negative control ES cells. ES cell clones indicated by *arrows* showed marked reduction in SOD1 production. *B*, detection of the antisense strand of siRNA in the brain on Northern blot analysis. *C*, SOD1 mRNA on Northern blot analysis in the brain. *D*, SOD1 protein on Western blot analysis in the brain. *E*, the presence of SOD1 in the spinal cord, as detected by immunohistochemistry (*upper panels*). *Lower panels*, the same sections stained with hematoxylin and eosin. *Scale bar*, 30 μm. *Tg*, anti-SOD1 siRNA Tg mouse; *Wt*, wild-type littermate.

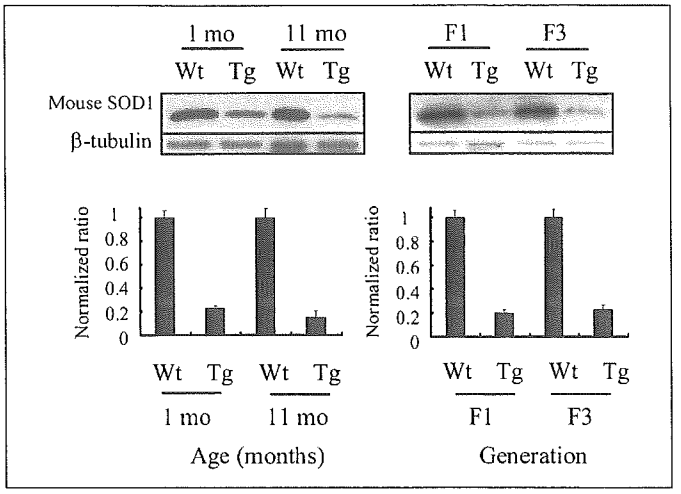

FIGURE 3. **The silencing effect of siRNA is stable.** SOD1 protein levels with aging (*left*) and from generation to generation (*right*) are shown. F1 and F3 mice were examined at 1 month (*mo*) of age. Values are the ratios to age-matched wild-type (*Wt*) littermates (mean and S.E.). $n = 3$ for each group. *ns* = not significant ($p > 0.05$, Student's t test).

antibody S-100 (1:1000, StressGen Biotechnologies). Staining was visualized by diaminobenzidine. For histopathological examination of the tissues of double Tg mice, SOD1^{G93A} Tg mice, and wild-type littermates, sections 10 μm thick were stained with hematoxylin and eosin.

L3 ventral roots were taken from the spinal cord and fixed in phosphate-buffered 2.5% glutaraldehyde, postfixed in 1% osmic acid, and then embedded in Epon. Toluidine blue-stained semi-thin transverse sections of these materials were used for evaluation of the density and size distribution of myelinated fibers.

Determination of Disease Onset and Progression—We compared the motor functions of double Tg mice with those of SOD1^{G93A} Tg mice and wild-type littermates by using a rotating rod apparatus (accelerating model, Ugo Basile Biological Research Apparatus, Varese, Italy). The mice were placed on the rod for four trials. Each trial lasted a maximum of 4 min, during which the rotating rod underwent linear acceleration from 4 to 33 rpm over 4 min. Disease onset was determined by the presence of hindlimb paresis on walking. Mortality was scored as date of death or inability of the mouse to right itself within 30 s of being placed on its side.

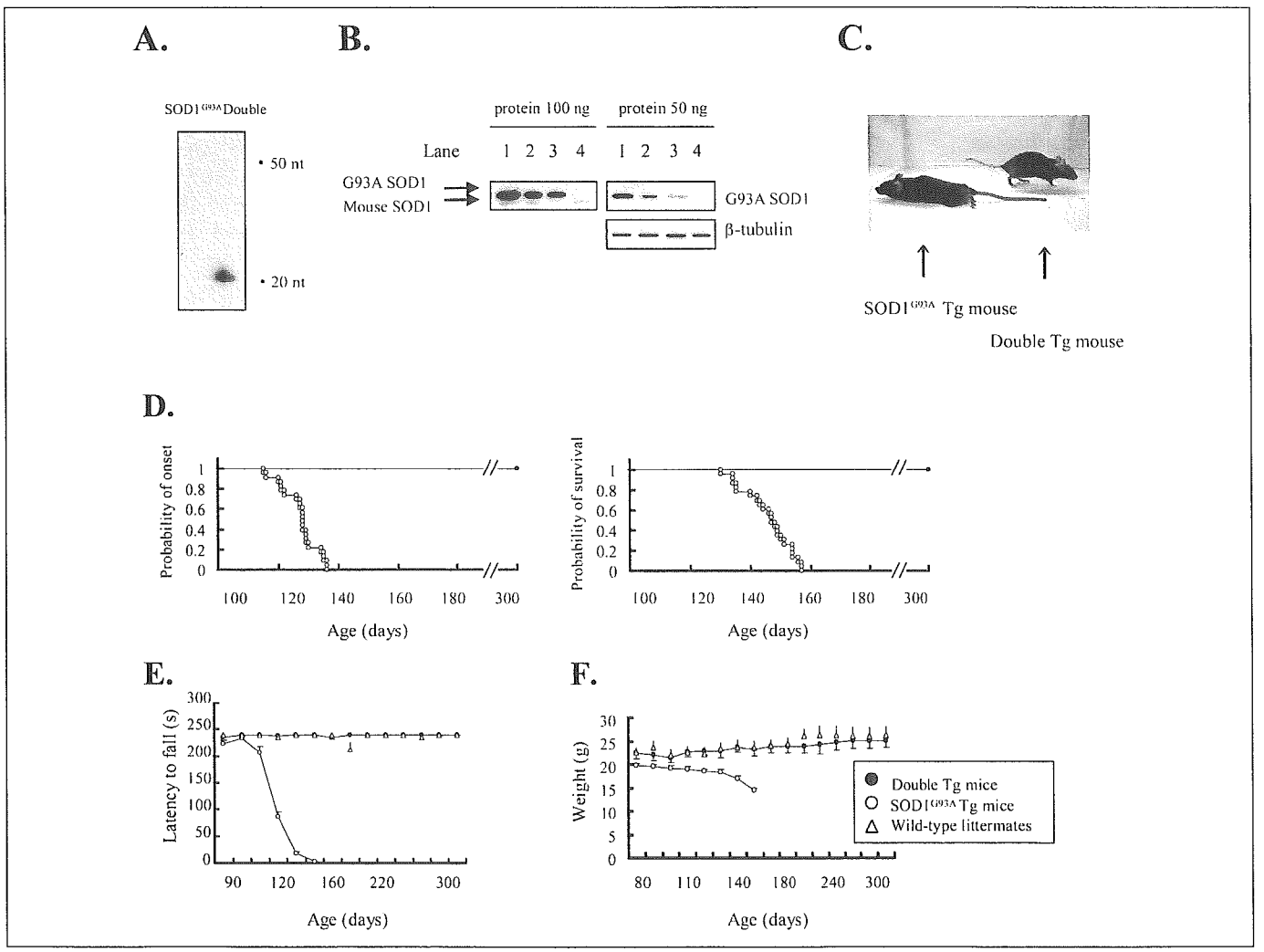

FIGURE 4. **Double Tg mice had a marked reduction in the amount of G93A SOD1 protein in the spinal cord and did not show the ALS phenotype.** *A*, detection of the antisense strand of siRNA in the spinal cord on Northern blot analysis. *nt*, nucleotides. *B*, levels of both mutant G93A SOD1 and mouse SOD1 proteins were similarly reduced in the spinal cords of double Tg mice on Western blot analysis. The level of G93A SOD1 protein in double Tg mice was lower than that of the low copy strain of SOD1^{G93A} Tg mice. *Lane 1*, SOD1^{G93A} Tg mouse; *lane 2*, low copy strain of SOD1^{G93A} Tg mouse; *lane 3*, double Tg mouse; *lane 4*, wild-type mouse. *C*, this SOD1^{G93A} Tg mouse at 130 days of age showed paralysis of both hindlimbs. In contrast, the double Tg mouse at the same age walked well. *D*, cumulative probabilities of onset of disease signs (*left*) and survival (*right*). There was a significant increase in the life span of the double Tg mice ($n = 6$; *closed circles*) compared with the SOD1^{G93A} Tg mice ($n = 23$; *open circles*). *E*, performances on the accelerating rotating rod apparatus. *F*, growth curves of female mice. Values are means and S.E.

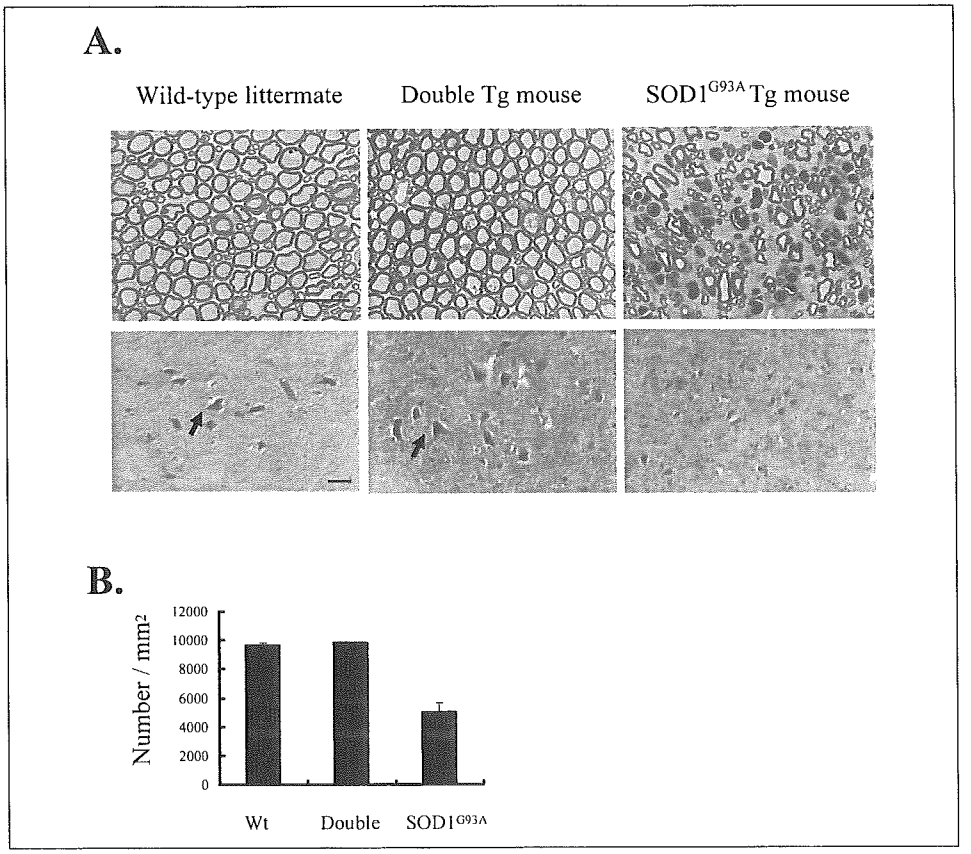

FIGURE 5. **Histological analysis of lumbar ventral root and spinal cord.** *A*, light micrographs of transverse L3 ventral root sections stained with toluidine blue (*upper panels*) and L3 spinal cords stained with hematoxylin and eosin (*lower panels*). The *arrows* indicate the anterior horn cells. *Scale bar*, 30 μm. *B*, the number of large motor fibers (≥5 μm) in L3 ventral roots. Values are means and S.E. $n = 3$ for wild-type littermates and SOD1^{G93A} Tg mice; $n = 1$ for double Tg mice.

Statistical Analysis—Statistical significance was assessed between groups by using Student's *t* test. Significance was set at $p < 0.05$.

RESULTS

Anti-SOD1 siRNA Tg Mice—We obtained 3 of 50 G418-resistant ES cell clones that showed an ~80% reduction in the level of endogenous SOD1 protein by Western blot analysis (Fig. 2*A*). Each ES cell clone was injected into C57BL/6 blastocysts, and chimeric male mice with high levels of ES cell descendants were obtained. These chimeras were outcrossed, and germline transmission of the shRNA was noted in numerous F1 progeny from one ES line (12/35) on PCR analysis. In the brains of anti-SOD1 siRNA Tg mice, expression of siRNA was clearly detected (Fig. 2*B*), and mouse SOD1 mRNA was strikingly reduced on Northern blot analysis (Fig. 2*C*). The level of SOD1 protein was also suppressed by about 80% on Western blot analysis (Fig. 2*D*). Anti-SOD1 siRNA Tg mice did not show any obvious phenotype such as growth retardation or motor signs, with the exception of infertility in females. In immunohistochemical analysis, the SOD1 immunoreactivity of both the gray and the white matter of the spinal cord in the anti-SOD1 siRNA Tg mice was much lower than that in the wild-type littermates. In the anterior horn of the spinal cord in anti-SOD1 siRNA Tg mice, the SOD1 immunoreactivity was reduced dominantly in the non-neuronal cells and neuropils (Fig. 2*E*).

The Silencing Effect of siRNA Is Stable with Age and through to the F3 Generation—To analyze changes in SOD1 protein levels with age and through the generations, we examined SOD1 protein levels in the tails of anti-SOD1 siRNA Tg mice and age-matched wild-type littermates by Western blot analysis. There was no obvious decrease in the effect of siRNA on knockdown of SOD1 production at 1 and 11 months old or in F1 and F3 mice (Fig. 3).

Mutant G93A SOD1 Protein Production Is Decreased in Double Tg Mice—By crossing anti-SOD1 siRNA Tg mice with SOD1^{G93A} Tg mice, we obtained six double Tg mice and 26 SOD1^{G93A} Tg mice. In the spinal cords of the double Tg mice, we clearly detected the expression of siRNA (Fig. 4*A*). Levels of both mutant human G93A SOD1 protein and mouse wild-type SOD1 protein in the spinal cords of the double Tg mice were similarly reduced. The percentage of reduction of mutant G93A SOD1 in the spinal cord was estimated to be about 80%. The level of mutant G93A SOD1 protein in the double Tg mice was about half that in the low copy strain of SOD1^{G93A} Tg mice (G1L/+ from Jackson Laboratories, backcrossed to C57BL/6 mice) in which disease onset occurred at 280 days of age (Fig. 4*B*).

Phenotype of Double Tg Mice Is Normal—SOD1^{G93A} Tg mice showed the first signs of motor deficits at a mean age of 127.3 ± 1.2 days. All of these mice then deteriorated progressively, showing a lack of mobility, failure to groom their fur, hindlimb dysfunction, breathing difficulties, and muscle atrophy. All SOD1^{G93A} Tg mice were dead by 157 days of age (Fig. 4, *C* and *D*).

In contrast, double Tg mice appeared normal and grew up similarly to wild-type littermates. Their motor performance on the rotating rod test did not differ from that of wild-type littermates over the entire 300-day duration of the experiment (Fig. 4*E*). The weights of SOD1^{G93A} Tg mice declined just before the onset of disease, but double Tg mice did not lose weight (Fig. 4*F*). The online supplemental movie dramatically shows that the transgenic anti-SOD1 siRNA completely prevented the development of the ALS phenotype seen in SOD1^{G93A} Tg mice (see Supplemental Movie).

Histological analysis of the spinal cord was performed at the end of disease in SOD1^{G93A} Tg mice and at 6 months of age in double Tg mice and the age-matched wild-type littermates. In the SOD1^{G93A} Tg mice,

the spinal cord at L3 showed a severe loss of motor neurons with an increase in the numbers of astrocytes (see Supplemental Figure), and myelinated axons in the L3 ventral root were atrophic and less dense. In contrast, the spinal motor neurons and axons in the double Tg mice appeared normal (Fig. 5, *A* and *B*).

DISCUSSION

One serious problem in using shRNA to generate Tg mice is that mutations can occur within the hairpin region of the shRNA sequence during replication, leading to a reduction in silencing efficiency with age and over generations. In fact, ~20% of our constructs without mismatch alternation were mutated within the hairpin region of the constructs upon introduction into *Escherichia coli* (8), and some anti-green fluorescent protein Tg mice lost the knockdown effect in the F1 generation, even with expression of siRNA (9). We previously showed that mismatch alternation of a few nucleotides in only the sense strand prevented mutation during replication without reducing the silencing effect (8). Thus, we introduced three mismatch alternations in the sense strand, and all of our anti-SOD1 Tg mice showed no decrease in siRNA effect over four generations. The mismatch alternations in the sense strand of our shRNA might have prevented a decrease in the siRNA effect *in vivo*. In view of these results, we think that crossing of siRNA Tg mice could be a useful strategy for analyzing the effect of knockdown of the gene of interest on the phenotype of the crossed mice.

Our results showed that development of the ALS phenotype in $SOD1^{G93A}$ Tg mice was completely suppressed by crossing with anti-SOD1 siRNA Tg mice. In our double Tg mice, siRNA overexpressed against the *SOD1* gene in anti-SOD1 siRNA Tg mice cleaved the mRNA of G93A SOD1 expressed in the crossed mice. We consider that prevention of development of the ALS phenotype in the double Tg mice was caused by the knockdown effect on SOD1 protein production. The mouse wild-type *SOD1* gene was similarly inhibited by the siRNA, but elimination of wild-type SOD1 has been reported to have no effect on the mutant SOD1-mediated ALS phenotype (10). An off-target effect of the siRNA on other unidentified mouse genes is also improbable. This is because 1) a BLAST search for our shRNA sequence showed no match in other areas of the mouse genome and 2) the infertility observed in female anti-SOD1 siRNA Tg mice has also been reported in mice with knock-out of the *SOD1* gene (11). Moreover, a close relationship between the copy number of G93A SOD1 and time of onset of the ALS phenotype is known to occur in $SOD1^{G93A}$ Tg mice (12).

More recently, direct injection of an siRNA-expressing viral vector into the spinal cord (5) or skeletal muscles (6, 7) is reported to reduce the severity of the ALS phenotype in $SOD1^{G93A}$ Tg mice. Although viral vector-mediated siRNA delayed the onset of disease or the decrease in grip strength, none of these vector-mediated siRNAs could prevent the disease. In contrast, our double Tg mice did not show any motor dysfunction at 300 days and were expected to remain free of signs of disease at 2 years of age, the time at which disease onset has been predicted from the rate of reduction in the amount of mutant SOD1 in the spinal cord (12). Most likely, this difference can be explained by the possibility that our transgenic siRNA had a greater knockdown effect than did the viral vector-mediated siRNA. Alternatively, reduction in the amount of mutant SOD1 in non-neuronal cells as well as neuronal cells in our double Tg mice might have contributed to the better outcome; the effects of siRNA were limited to the motoneurons when viral vectors were injected into the skeletal muscles (6, 7). There are several lines of evidence that production of mutant SOD1 in both neuronal and non-neuronal cells is critical in the mechanism of the disease (13–16).

Our findings clearly demonstrated that siRNA halted familial ALS by silencing the mutant gene. If a non-invasive method of delivery of siRNA to both neuronal and non-neuronal cells throughout the central nervous system can be developed, the concept of truly overcoming these autosomal dominantly inherited neurodegenerative diseases will no longer be an impossibility.

Acknowledgments—We thank Dr. Ryosuke Takahashi (Kyoto University) and Dr. Hideki Nishitoh (Tokyo Medical and Dental University) for providing the transgenic animals and Dr. Taro Hino, Dr. Yoichiro Nishida, Dr. Hiroki Sasaguri, Satoshi Ikeda, Tsubura Takahashi, and Hiromi Yamada (Tokyo Medical and Dental University) for help.

REFERENCES

1. Rosen, D. R., Siddique, T., Patterson, D., Figlewicz, D. A., Sapp, P., Hentati, A., Donaldson, D., Goto, J., O'Regan, J. P., Deng, H.-X., Rahmani, Z., Krizus, A., McKenna-Yasek, D., Cayabyab, A., Gaston, S. M., Berger, R., Tanzi, R. E., Halperin, J. J., Herzfeldt, B., Van den Bergh, R., Hung, W.-Y., Bird, T., Deng, G., Mulder, D. W., Smyth, C., Laing, N. G., Soriano, E., Pericak-Vance, M. A., Haines, J., Rouleau, G. A., Gusella, J. S., Horvitz, H. R., and Brown, R. H., Jr. (1993) *Nature* **362,** 59–62
2. Cleveland, D. W. (1999) *Neuron* **24,** 515–520
3. Yokota, T., Miyagishi, M., Hino, T., Matsumura, R., Andrea, T., Urushitani, M., Rao, R. V., Takahashi, R., Bredesen, D. E., Taira, K., and Mizusawa, H. (2004) *Biochem. Biophys. Res. Com.* **314,** 283–291
4. Xia, H., Mao, Q., Eliason, S. L., Harper, S. Q., Martins, I. H., Orr, H. T., Paulson, H. L., Yang, L., Kotin, R. M., and Davidson, B. L. (2004) *Nat. Med.* **10,** 816–820
5. Raoul, C., Abbas-Terki, T., Bensadoun, J.-C., Guillot, S., Haase, G., Szulc, J., Henderson, C. E., and Aebischer, P. (2005) *Nat. Med.* **11,** 423–428
6. Ralph, G. S., Radcliffe, P. A., Day, D. M., Carthy, J. M., Leroux, M. A., Lee, D. C. P., Wong, L.-F., Bilsland, L. G., Greensmith, L., Kingsman, S. M., Mitrophanous, K. A., Mazarakis, N. D., and Azzouz, M. (2005) *Nat. Med.* **11,** 429–433
7. Miller, T. M., Kasper, B. K., Kops, G. J., Yamanaka, K., Christian, L. J., Gage, F. H., and Cleveland, D. W. (2005) *Ann. Neurol.* **57,** 773–776
8. Miyagishi, M., Sumimoto, H., Miyoshi, H., Kawakami, Y., and Taira, K. (2004) *J. Gene Med.* **6,** 715–723
9. Hasuwa, H., and Okabe, M. (2003) *Gene Medicine (Tokyo)* **7,** 59–64
10. Bruijn, L. I., Houseweart, M. K., Kato, S., Anderson, K. L., Anderson, S. D., Ohama, E., Reaume, A. G., Scott, R. W., and Cleveland, D. W. (1998) *Science* **281,** 1851–1854
11. Matzuk, M. M., Dionne, L., Guo, Q., Kumar, T. R., and Lebovitz, R. M. (1998) *Endocrinology* **139,** 4008–4011
12. Alexander, G. M., Erwin, K. L., Byers, N., Deitch, J. S., Augelli, B. J., Blankenhorn, E. P., and Heiman-Patterson, T. D. (2004) *Mol. Brain Res.* **130,** 7–15
13. Gong, Y. H., Parsadanian, A. S., Andreeva, A., Snider, W. D., and Elliott, J. L. (2000) *J. Neurosci.* **20,** 660–665
14. Lino, M. M., Schneider, C., and Caroni, P. (2002) *J. Neurosci.* **22,** 4825–4832
15. Raoul, C., Estevez, A., Nishimune, H., Cleveland, D. W., deLapeyriere, O., Henderson, C. E., Haase, G., and Pettmann, B. (2002) *Neuron* **35,** 1067–1083
16. Clement, A. M., Nguyen, M. D., Roberts, E. A., Garcia, M. L., Boillee, S., Rule, M., McMahon, A. P., Doucette, W., Siwek, D., Ferrante, R. J., Brown, R. H., Jr., Julien, J. P., Goldstein, L. S., and Cleveland, D. W. (2003) *Science* **302,** 113–117

Journal of Neurochemistry, 2005, **93**, 63–71 doi:10.1111/j.1471-4159.2004.02994.x

Selective gene silencing of rat ATP-binding cassette G2 transporter in an *in vitro* blood–brain barrier model by short interfering RNA

Satoko Hori,*·†·¶ Sumio Ohtsuki,*·†·¶ Masashi Ichinowatari,* Takanori Yokota,‡ Takashi Kanda‡ and Tetsuya Terasaki*·†·¶

**Department of Molecular Biopharmacy and Genetics, Graduate School of Pharmaceutical Sciences, Tohoku University, Sendai, Japan*

†New Industry Creation Hatchery Center, Tohoku University, Sendai, Japan

¶CREST and SORST of the Japan Science and Technology Agency (JST), Japan

‡Department of Neurology and Neurological Science, Graduate School of Medicine, Tokyo Medical and Dental University, Tokyo, Japan

Abstract

The aim of the present study was to specifically silence the rat ATP-binding cassette transporter G2 (rABCG2) gene in brain capillary endothelial cells by transfection of short interfering RNA (siRNA). Four different siRNAs designed to target rABCG2 were each transfected into HEK293 cells with myc-tagged rABCG2 cDNA. Quantitative real-time PCR and western blot analyses revealed that three of the siRNAs were able to reduce exogenous rABCG2 mRNA and protein levels in HEK293 cells. Moreover, rABCG2-mediated mitoxantrone efflux transport was suppressed by the introduction of these three siRNAs into HEK293 cells. In contrast, the other siRNA and non-specific control siRNA did not significantly affect the mRNA expression, the protein level or the transport activity. Endogenous rABCG2 mRNA and protein expression in a conditionally immortalized rat brain capillary endothelial cell line (TR-BBB13) was suppressed by the most potent siRNA among the four siRNAs tested. Furthermore, this siRNA did not affect the mRNA levels of other ABC transporters, such as ABCB1, ABCC1 and ABCG1, and the protein level of ABCB1 in TR-BBB13 cells, suggesting that it can selectively silence rABCG2 at the blood–brain barrier. This should be a useful and novel strategy for clarifying the contribution of rABCG2 to brain-to-blood transport of substrate drugs and endogenous compounds across the blood–brain barrier.

Keywords: ABC transporter, ATP-binding cassette transporter G2, 17β-estradiol, blood–brain barrier, *in vitro* blood–brain barrier model, short interfering RNA.

J. Neurochem. (2005) **93**, 63–71.

The blood–brain barrier (BBB), which is formed by the tight intercellular junctions of brain capillary endothelial cells (BCECs), strictly regulates the transfer of substances between the circulating blood and the brain (Terasaki and Hosoya 1999; Hosoya *et al.* 2002). Therefore, the molecular mechanisms of efflux transport from the brain have important implications for drug delivery and CNS homeostasis.

ABCG2 (BCRP/MXR/ABCP1) is an ATP-binding cassette (ABC) transporter localized on the luminal side of brain capillaries in humans (Cooray *et al.* 2002) and rats (Hori *et al.* 2004), and transports a diverse array of compounds out of the cells (Allen and Schinkel 2002). Therefore, ABCG2 present in BCECs may act to restrict the penetration of xenobiotics into the brain and to pump out potential toxins or metabolites from the brain. ABCG2 transports sulfated conjugates of drugs and sterols (Suzuki *et al.* 2003), whereas p-glycoprotein (P-gp), a well-characterized efflux transporter at the BBB, preferentially transports hydrophobic

Received May 10, 2004; revised manuscript received November 16, 2004; accepted November 17, 2004.

Address correspondence and reprint requests to Tetsuya Terasaki, Department of Molecular Biopharmacy and Genetics, Graduate School of Pharmaceutical Sciences, Tohoku University, Aoba, Aramaki, Aoba-ku, Sendai 980–8578, Japan. E-mail: terasaki@mail.pharm.tohoku.ac.jp

Abbreviations used: ABC, ATP-binding cassette; BBB, blood–brain barrier; BCEC, brain capillary endothelial cell; DHEAS, dehydroepiandrosterone sulfate; NC, non-specific control; PMSF, phenylmethylsulphonyl fluoride; SDS–PAGE, sodium dodecyl sulfate polyacrylamide gel electrophoresis; siRNA, short interfering RNA; TR-BBB, conditionally immortalized brain capillary endothelial cell line.

compounds. Therefore, ABCG2 may have a distinct role in efflux transport at the BBB.

Several ABC transporters and organic anion transporters are expressed at the abluminal and/or luminal membrane of the BBB as well as ABCG2 (Gao *et al.* 1999; Virgintino *et al.* 2002; Mori *et al.* 2003). Clarifying the transport properties and the contribution of each transporter at the BBB is an important issue for understanding the physiological roles of these molecules. However, the substrate and inhibitor specificities of these transporters sometimes overlap. For example, dehydroepiandrosterone sulfate (DHEAS) is transported from brain to the circulating blood across the BBB via organic anion transporting polypeptide 2 (Asaba *et al.* 2000), while other transporters at the BBB, such as ABCG2 and ABCC4 (Zhang *et al.* 2000; Cooray *et al.* 2002; Hori *et al.* 2004), also accept DHEAS as a substrate (Suzuki *et al.* 2003; Zelcer *et al.* 2003).

Three effective inhibitors of ABCG2 have been described thus far. GF120918 was developed as a P-gp (ABCB1) inhibitor (Hyafil *et al.* 1993), but a later study found that it also inhibits ABCG2 (de Bruin *et al.* 1999). Such a dual-specificity inhibitor is unsuitable for clarifying the distinct transport activity of each transporter. Fumitoremorgin C and Ko143 are potent and selective inhibitors for ABCG2, being much less active towards P-gp and ABCCs (Rabindran *et al.* 2000; Allen *et al.* 2002). Nevertheless, the specificity of these inhibitors is concentration-dependent, and an influence of these two inhibitors on unidentified transporters at the BBB cannot be ruled out.

RNA interference is a conserved biological response to double-stranded RNA, which results in sequence-specific gene silencing (Hannon 2002). In mammalian cell cultures, double-stranded RNA-mediated interference with gene expression has also been accomplished by transfection of synthetic RNA oligonucleotides composed of 21 or 22 base pairs (short interfering RNA, siRNA; Elbashir *et al.* 2002). Sequence-specific silencing of transporter genes using siRNA should make it possible to evaluate properly the transport properties of a targeted transporter at the BBB.

Conditionally immortalized BCEC lines are useful *in vitro* BBB models which retain the *in vivo* transport properties towards various compounds (Hosoya *et al.* 2000a, 2000b; Terasaki *et al.* 2003). Endothelial cells are generally resistant to the introduction of exogenous DNA, and molecular analysis of endothelial cells has been hampered by the difficulty of transiently transfecting genes with high efficiency. Therefore, siRNA-induced specific knockdown of target transporter genes in BCECs should allow us to improve our understanding of the physiological and pharmacological functions of the efflux transport systems at the BBB.

The purpose of this study was therefore to specifically silence rABCG2 gene by the introduction of siRNA into BCECs, in order to clarify the role of ABCG2 at the BBB.

Materials and methods

Reagents

Endothelial cell growth factor (ECGF) was purchased from Boehringer Mannheim (Mannheim, Germany). Benzylpenicillin potassium and streptomycin sulfate were purchased from Wako Pure Chemical Industries (Osaka, Japan). Non-specific Control Duplex XI (NC siRNA; Dharmacon, Lafayette, CO, USA) is claimed by the manufacturer to show no RNAi effect, and its target sequence is 5′-NNATAGATAAGCAAGCCTTAC-3′. No rat gene sequences with homology to NC siRNA were found by Blast search. β-Actin siRNA was purchased from Qiagen (Tokyo, Japan); its target sequence is 5′-AATGAAGATCAAGATCATTGC-3′. The sequence of β-actin siRNA is identical at 20 bp out of 21 bp with the corresponding sequence of rat β-actin (the underlined base in the sequence of β-actin siRNA is changed to 'C' in that of rat β-actin). All other chemicals were commercial products of analytical grade.

siRNA preparation

Four different siRNA duplexes were designed based on the coding sequence of rABCG2 cDNA (GenBank accession number AB105817). All 21-nucleotides (nt) siRNAs contained 3′-dTdT extensions and their GC contents were less than 70%. The sequences, positions and GC contents of siRNA targeting rat ABCG2 are shown in Table 1. All of the siRNA duplexes were

Table 1 Sequences of rABCG2 short interfering RNAs (siRNAs)

Number of rABCG2 siRNA	Sequences (upper, sense; lower, antisense)	Positions*/GC (%)
01	5′-CAGAGAAACAAGAACGGCCdTdT dTdTGUCUCUUUGUUCUUGCCGG-5′	95–113/52.6%
02	5′-UGUGCUAAGUUUUCAUCACdTdT dTdTACACGAUUCAAAAGUAGUG-5′	160–178/36.8%
03	5′-CCCUGACAGUGAGAGAAAAdTdT dTdTGGGACUGUCACUCUCUUUU-5′	450–468/47.4%
04	5′-GCAAACAAGACAGAAGAGCdTdT dTdTCGUUUGUUCUGUCUUCUCG-5′	998–1016/47.4%

*GenBank accession number AB105817.

chemically synthesized and HPLC-purified by Proligo (La Jolla, CA, USA).

Cell culture

HEK293 cells (American Type Culture Collection, Rockville, MD, USA) were grown in Dulbecco's modified Eagle's medium (DMEM, Nissui Pharmaceutical, Tokyo, Japan) supplemented with 20 mM sodium bicarbonate, 100 U/mL benzylpenicillin potassium, 100 μg/mL streptomycin sulfate and 10% fetal bovine serum (Moregate, Bulimba, Australia; culture-medium A) at 37°C in a humidified atmosphere of 95% air and 5% CO_2. TR-BBB13 cells are a conditionally immortalized BCEC cell line (Hosoya *et al.* 2000a) that has been used as an *in vitro* BBB model (Terasaki *et al.* 2003). TR-BBB13 cells were grown in culture-medium A with 15 ng/mL ECGF. The cells were maintained at 33°C, which is a permissive temperature at which temperature-sensitive SV40 large T-antigen is activated, in a humidified atomosphere of 95% air and 5% CO_2.

Transfection of siRNA into HEK293 cells or TR-BBB13 cells

HEK293 cells were plated in six-well plates at 4×10^5 cells/well, grown for 24 h then transfected with 3 μg of rABCG2 siRNA-01, rABCG2 siRNA-02, rABCG2 siRNA-03, rABCG2 siRNA-04 or NC siRNA using Lipofectamine 2000 and OPTI-MEM I reduced serum medium (Invitrogen, Carlsbad, CA, USA). In some experiments, 1 μg of myc-tagged rABCG2 cDNA (pCMV-Tag3A/rABCG2 (Hori *et al.* 2004)) or a control plasmid (pCMV-Tag3A, Stratagene, La Jolla, CA, USA) was co-transfected into HEK293 cells simultaneously with siRNA. The mRNA expression and the transport activity were examined at 48 h after the transfection. The protein expression was examined at 24, 48 and 72 h after the transfection.

For quantitative real-time PCR analysis, TR-BBB13 cells were plated in six-well plates at 4×10^5 cells/well, grown for 24 h at 33°C then transfected with 4 μg of rABCG2 siRNA-03, β-actin siRNA or NC siRNA using Lipofectamine 2000 and OPTI-MEM I reduced serum medium (Invitrogen). At 24 h after siRNA transfection, TR-BBB13 cells were treated with or without 100 nM 17β-estradiol. Culture was continued for a further 24 h at 33°C. For western blot analysis, TR-BBB13 cells were plated in six-well plates at 4×10^5 cells/well, grown for 24 h at 33°C then transfected with 4 μg of rABCG2 siRNA-03 or NC siRNA using Lipofectamine 2000 and OPTI-MEM I reduced serum medium (Invitrogen). The protein expression was examined at 36 h after the transfection.

Quantitative real-time PCR analysis

Total RNA was extracted from HEK293 cells or TR-BBB13 cells with an RNeasy kit (Qiagen) according to the manufacturer's protocol. RNA integrity was checked by electrophoresis on an agarose gel. Single-stranded cDNA was prepared from 1 μg of total RNA by RT (ReverTraAce, Toyobo, Osaka, Japan) using oligo dT primer. Quantitative real-time PCR analysis was performed using an ABI PRISM 7700 sequence detector system (PE Applied Biosystems, Foster City, CA, USA) with 2 × SYBR Green PCR Master Mix (PE Applied Biosystems) according to the manufacturer's protocol. To quantify the amount of specific mRNA in the samples, standards for each run were prepared using pGEM-T Easy Vector containing ABCG2, ABCB1, ABCC1, ABCG1, β-actin or GAPDH (dilution ranging from 0.1 fg/μL to 1 ng/μL). The standard curves of each gene were obtained by linear regression between the logarithm of the standards of each gene and the corresponding threshold cycle (Ct) values. The Ct value indicates the cycle number at which the reaction begins to be exponential. All the plots showed high linearity, and the Ct values of all samples were within the range of the standard plots. The ABCG2, ABCB1, ABCC1 or ABCG1 mRNA levels were normalized relative to the β-actin mRNA level. The β-actin mRNA level was normalized relative to the GAPDH mRNA level. In Fig. 1, each rABCG2 mRNA level is indicated as a percentage of the mean of those in HEK293 cells co-transfected with NC siRNA and rABCG2 cDNA ($n = 3$; open column, NC+). In Fig. 4, each mRNA level is indicated as a percentage of the mean of mRNA levels in TR-BBB13 cells treated with non-siRNA (–) and 17β-estradiol (E2; $n = 3$; the leftmost column). The control lacking the RT enzyme was assayed in parallel to monitor any possible genomic contamination. The PCR was run for 40 cycles of 95°C for 30 s, 60°C for 1 min, and 72°C for 1 min after pre-incubation at 95°C for 10 min, using specific primers. The sequences of primers were as follows: sense primer 5′-CAATGGGATCATGAAACC-TG-3′, antisense primer 5′-GAGGCTGATGAATGGAGAA-3′ for ABCG2; sense primer 5′-ACAGAAACAGAGGATCGC-3′ and antisense primer 5′-CGTCTTGATCATGTGGCC-3′ for ABCB1/mdr1a; sense primer 5′-CTGGCTTGGTGTGAACTGAT-3′ and antisense primer 5′-AGGCTCTGGCTTGGCTCTAT-3′ for ABCC1; sense primer 5′-TGCCCGCCGGGTTGAAACTGTTC-3′ and antisense primer 5′-ACTGTCTGCATTGCGTTGCATTGC-3′ for ABCG1; sense primer 5′-TTTGAGACCTTCAACACCCC-3′ and

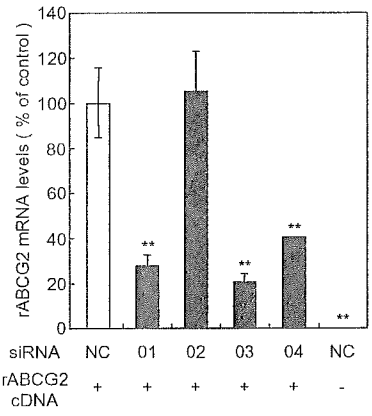

Fig. 1 Effects of rABCG2 siRNAs on the exogenous rABCG2 mRNA level in HEK293 cells co-transfected with myc-tagged rABCG2 cDNA. HEK293 cells were transfected with siRNAs (rABCG2 siRNA-01, rABCG2 siRNA-02, rABCG2 siRNA-03 and rABCG2 siRNA-04 (01, 02, 03 and 04) or non-specific control (NC) siRNA) with (+) or without (–) co-transfection of myc-tagged rABCG2 cDNA. At 48 h after transfection, the cells were collected for quantitative real-time PCR analysis. The sequences of rABCG2 siRNAs are shown in Table 1. Each column represents the mean ± SEM ($n = 3$). The rABCG2 mRNA level was normalized relative to the β-actin mRNA level. Each rABCG2 mRNA level is shown as percentage of the mean of the rABCG2 mRNA level in the NC siRNA-treated HEK293 cells cotransfected with myc-tagged rABCG2 cDNA (NC+). $^{**}p < 0.01$, significantly different from the NC+.

antisense primer 5′-ATAGCTCTTCTCCAGGGAGG-3′ for β-actin; sense primer 5′-TGATGACATCAAGAAGGTGGTGAAG-3′ and antisense primer 5′-TCCTTGGAGGCCATGTAGGCCAT-3′ for GAPDH.

Western blot analysis

HEK293 cells were lysed with lysis buffer containing 10 mM Tris–HCl (pH 7.4), 1 mM EDTA, 150 mM NaCl, 4% CHAPS, 1 mM phenylmethylsulfonyl fluoride, and a protease-inhibitor cocktail (Sigma Chemical Co., St Louis, MO, USA). The lysate was centrifuged at 15 000 *g* for 30 min and the supernatants were collected. TR-BBB13 cells were homogenized by mean of the nitrogen cavitation technique (800 psi, 15 min, 4°C) in buffer containing 10 mM HEPES-NaOH (pH 7.4), 250 mM sucrose, 1 mM EDTA, 1 mM phenylmethylsulphonyl fluoride (PMSF). The homogenized samples were centrifuged at 10 000 *g* for 10 min and the supernatants were collected. These supernatants were centrifuged at 100 000 *g* for 1 h, and a crude membrane fraction was obtained from the pellets. The pellets were suspended in lysis buffer. The protein concentration of samples was measured by the Bradford method using Bio-Rad Protein Assay reagent (Bio-Rad, Hercules, CA, USA). Protein samples (HEK293 cells, 12 μg; TR-BBB13 cells, 40 μg (for rABCG2) or 20 μg (for Na^+,K^+-ATPase and ABCB1) per lane) were resolved by 7.5% sodium dodecyl sulfate polyacrylamide gel electrophoresis (SDS–PAGE; Bio-Rad) and subsequently electrotransferred to nitrocellulose membranes. Membranes were treated with blocking buffer (4% skimmed milk in 25 mM Tris–HCl (pH 8.0), 125 mM NaCl, 0.1% Tween-20 for 2 h at 20°C and incubated with anti-c-myc antibody (0.1 μg/mL; Bethyl Laboratories Inc., Montgomery, TX, USA), anti-β-actin antibody (1 : 2000; Sigma), anti-Na^+,K^+-ATPase antibody (0.1 μg/mL; Upstate Biotechnology, Lake Placid, NY, USA), anti-ABCB1 antibody (C219) (1 : 100; Signet, Dedham, MA, USA), or anti-ABCG2 antibody (G2-Ab1) (1.0 μg/mL) (Hori *et al.* 2004) as the primary antibody at 4°C for 16 h after blocking. The membranes were washed three times with blocking buffer and incubated with horseradish peroxidase-conjugated second antibody. The bands were visualized with an enhanced chemiluminescence kit (SuperSignal; Pierce, Rockford, IL, USA). The relative densities of the bands were measured using NIH image software (National Institutes of Health, Bethesda, MD, USA).

Transport assay

For transport studies, HEK293 cells were incubated for 1 h at 37°C in a medium containing 20 μM mitoxantrone. The cells were then washed in ice-cold phosphate-buffered saline and placed on ice until measurement. Relative cellular accumulation of mitoxantrone was determined by flow cytometry with a 635 nm red diode laser and 661 nm bandpass filter (FACs Calibur, BD Biosciences, Lexington, KY, USA). A total of 20 000 events were collected. Debris was eliminated by gating on forward versus side scatter. The mean channel number for each histogram was used as a measure of drug fluorescence for calculation.

Data analysis

Unless otherwise indicated, all data represent the mean ± SEM. An unpaired, two-tailed Student's *t*-test was used to determine the significance of differences between two group means. One-way ANOVA followed by the modified Fisher's least-squares difference method was used to assess the statistical significance of differences among means of more than two groups.

Results

Silencing of exogenous rABCG2 gene in HEK293 cells

To determine the effects of four different siRNAs (rABCG2 siRNA-01, rABCG2 siRNA-02, rABCG2 siRNA-03 and rABCG2 siRNA-04; Table 1) on rABCG2 gene expression, quantitative real-time PCR analysis was performed using HEK293 cells co-transfected with myc-tagged rABCG2 cDNA. After treatment with rABCG2 siRNA-01, rABCG2 siRNA-03 or rABCG2 siRNA-04 for 48 h, the rABCG2 mRNA levels were suppressed in rABCG2-transfected HEK293 cells by 71.8%, 78.8% or 54.7%, respectively (01+, 03+ and 04+, Fig. 1), compared with those in cells treated with non-specific control (NC) siRNA (NC+, Fig. 1). In contrast, treatment with rABCG2 siRNA-02 had no significant effect on the rABCG2 mRNA level (02+, Fig. 1).

Effects of siRNAs on rABCG2 protein level in HEK293 cells

To clarify whether rABCG2 protein was reduced concomitantly with the suppression of rABCG2 mRNA, the level of exogenous rABCG2 protein was examined by western blot analysis. The protein was detected using anti-c-myc antibody, as rABCG2 protein was fused with the myc epitope. Myc tagged-rABCG2 proteins were detected at 80 kDa in HEK293 cells co-transfected with NC siRNA and myc-tagged rABCG2 cDNA (NC+, Fig. 2a), while no band was detected in HEK293 cells co-transfected with NC siRNA and the vector alone (i.e. without the myc-tagged rABCG2 cDNA insert) (NC–, Fig. 2a). rABCG2 siRNA-01, rABCG2 siRNA-03 and rABCG2 siRNA-04 each reduced the level of rABCG2 protein in HEK293 cells co-transfected with myc-tagged rABCG2 cDNA (01+, 03+ and 04+, Fig. 2a). rABCG2 siRNA-03 was the most effective (03+, Fig. 2a), and it reduced the relative density of the bands by 99.7 ± 0.1% (mean ± SEM; $n = 3$) compared with NC siRNA. In contrast, the rABCG2 protein level was not affected by rABCG2 siRNA-02 (02+, Fig. 2a). The level of β-actin protein was unchanged by any of the rABCG2 siRNAs (Fig. 2a). As shown in Figs 2(b and c), western blot analysis at 24 h and 72 h after transfection clearly demonstrated that co-transfection of rABCG2 siRNA-03, but not NC siRNA, significantly reduced the level of rABCG2 protein.

Effects of rABCG2 siRNAs on mitoxantrone efflux transport in rABCG2 cDNA-transfected HEK293 cells

Mean fluorescence intensity of mitoxantrone was significantly reduced in HEK293 cells following co-transfection with NC siRNA and myc-tagged rABCG2 cDNA (NC+, Fig. 3a) compared with NC siRNA alone (NC–, Fig. 3a). The proportion of transiently rABCG2 cDNA-transfected cells was 25.7 ± 0.4% (mean ± SEM; $n = 3$; gated area, Fig. 3b). rABCG2 siRNA-01, rABCG2 siRNA-03 and rABCG2 siRNA-04 significantly increased the mean fluorescence intensity of mitoxantrone (01+, 03+ and 04+, Fig. 3a), and indeed, rABCG2 siRNA-03 completely reversed the reduction of the mitoxantrone level. Representative histogram and dot plots showed that the population of rABCG2-transfected cells almost completely

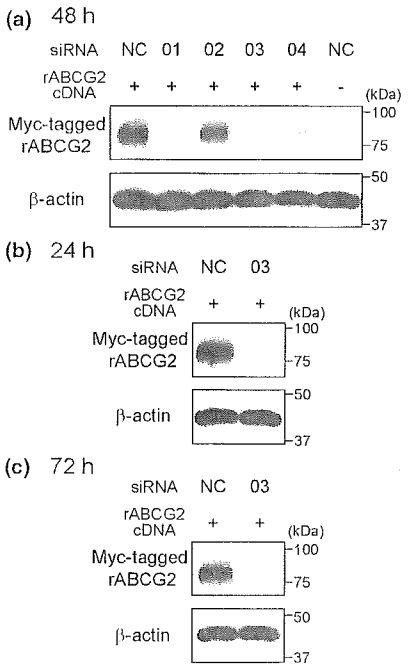

Fig. 2 Effects of rABCG2 siRNAs on exogenous rABCG2 protein in HEK293 cells co-transfected with myc-tagged rABCG2 cDNA. HEK293 cells were transfected with siRNAs (rABCG2 siRNA-01, rABCG2 siRNA-02, rABCG2 siRNA-03 and rABCG2 siRNA-04 (01, 02, 03 and 04) or non-specific control (NC) siRNA) with (+) or without (–) co-transfection of myc-tagged rABCG2 cDNA. The sequence of rABCG2 siRNAs are shown in Table 1. At 48 h (a), 24 h (b) or 72 h (c) after transfection, the cells were collected for western blot analysis using anti-c-myc and anti-β-actin antibodies. Typical results from repeated experiments are shown.

overlapped with that of non-transfected cells (03+, Fig. 3b). In contrast, rABCG2 siRNA-02 had no significant effect on the mean fluorescence intensity of mitoxantrone in HEK293 cells (02+, Fig. 3a).

Selective inhibition of endogenous rABCG2 gene in a conditionally immortalized BCEC line (TR-BBB13) by siRNA

rABCG2 siRNA-03, which is the most potent siRNA for attenuating rABCG2 function, was used to suppress endogenous rABCG2 expression in TR-BBB13 cells. At 24 h after siRNA transfection, TR-BBB13 cells were treated with 17β-estradiol, which has been reported to induce ABCG2 mRNA expression in cancer cells (Ee *et al.* 2004), or not treated. In the absence of 17β-estradiol, the rABCG2 mRNA level was reduced by 42.2% by transfection of rABCG2 siRNA-03 into TR-BBB13 cells (G2-03), whereas transfection of NC siRNA had no effect (NC)[E_2(–), Fig. 4a]. The rABCG2 mRNA level was significantly induced in non-siRNA-transfected TR-BBB13 cells following treatment with 17β-estradiol (open columns, Fig. 4a). The rABCG2 mRNA level was reduced by 75.7% by transfection of rABCG2 siRNA-03 into TR-BBB13 cells in the presence of 17β-estradiol (G2-03)[E_2(+), Fig. 4a]. In contrast, the transfection of NC siRNA did not affect the rABCG2 mRNA level in TR-BBB13 cells (NC)[E_2(+), Fig. 4a]. Treatment with siRNA targeted to β-actin decreased the β-actin mRNA level by 57.9 ± 2.2% (mean ± SEM; $n = 3$) in TR-BBB13 cells, supporting the view that siRNA was successfully transfected into TR-BBB13 cells.

To confirm the selectivity of the inhibitory effects of siRNA, the expression levels of other ABC transporters expressed in BCECs were examined. rABCG2 siRNA-03 did not significantly affect the ABCB1, ABCC1 and ABCG1 mRNA levels in TR-BBB13 cells in either the presence or absence of 17β-estradiol (Figs 4b–d). Following the 17β-estradiol treatment, the ABCB1 mRNA level was increased in TR-BBB13 cells (Fig. 4b), whereas the ABCC1 mRNA level showed a tendency to decrease (Fig. 4c), and the ABCG1 mRNA level was unchanged (Fig. 4d).

Suppression of endogenous rABCG2 protein expression in TR-BBB13 cells by siRNA

The rABCG2 protein expression was suppressed by transfection of rABCG2 siRNA-03 into TR-BBB13 cells (G2-03) compared with untransfected (–) and NC siRNA-transfected (NC) TR-BBB13 cells (Fig. 5a, upper panel). The expression of ABCB1 protein and Na^+,K^+-ATPase protein, used as a standard, was not changed by any of the treatment conditions (Fig. 5a, middle and lower panel, respectively). As shown in Fig. 5(b), the density ratio of rABCG2 to Na^+,K^+-ATPase density was significantly decreased by 62.1% by transfection of rABCG2 siRNA-03 into TR-BBB13 cells (G2-03) compared with untransfected TR-BBB13 cells (–).

Discussion

The present study demonstrated that introduction of any of three rABCG2 siRNAs efficiently decreased the expression of rABCG2 and suppressed the apparent efflux function of mitoxantrone, a substrate drug of rABCG2. Moreover, rABCG2 siRNA selectively suppressed the mRNA and protein expression of rABCG2 in a conditionally immortalized brain capillary endothelial cell line (TR-BBB), an *in vitro* BBB model.

Three of the siRNAs designed to target the rABCG2 gene induced sequence-specific suppression of the expression and function of the rABCG2 transporter (Figs 1–3). None of the siRNAs affected the β-actin protein levels (Fig. 2). This is the first evidence that rABCG2 function can be suppressed by siRNA-induced RNA interference. The differences in efficacy among these three siRNAs could be due to altered ability to silence the rABCG2 gene rather than altered transfection efficiency, because rABCG2 siRNA was present in about 900-fold molar excess over rABCG2-expression plasmid (the amount/length of the rABCG2 siRNA and the plasmid was 3 μg/21 bp and 1 μg/about 6300 bp, respectively). The protein expression and the transport activity of rABCG2 were completely suppressed at 48 h after rABCG2 siRNA-03 transfection (Figs 2 and 3), while reduction of the mRNA expression was around 80% (Fig. 1). This apparent difference may be because the protein level was below the detection threshold of western blot analysis, and below the level required for exerting its function. The expression of

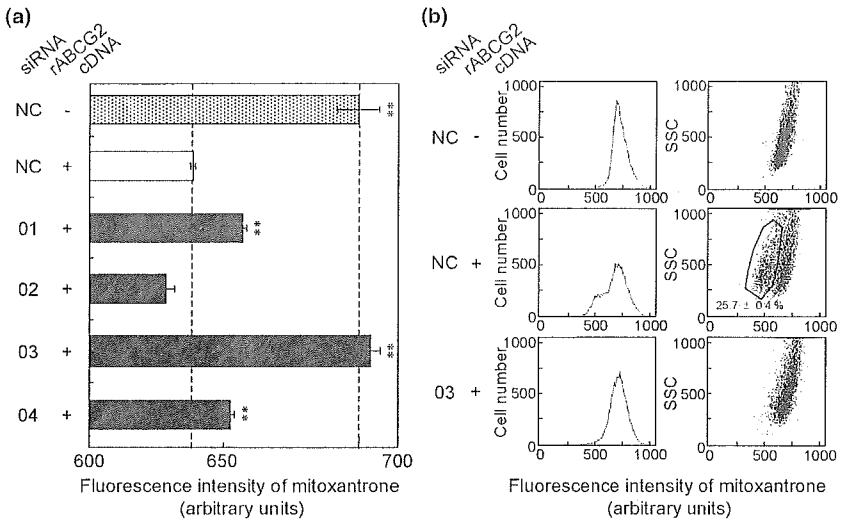

Fig. 3 Effects of rABCG2 siRNAs on mitoxantrone efflux transport in HEK293 cells co-transfected with myc-tagged rABCG2 cDNA. (a) HEK293 cells were transfected with siRNAs (rABCG2 siRNA-01, rABCG2 siRNA-02, rABCG2 siRNA-03 and rABCG2 siRNA-04 (01, 02, 03 and 04) or non-specific control (NC) siRNA) with (+) or without (–) cotransfection of myc-tagged rABCG2 cDNA. The sequences of rABCG2 siRNAs are shown in Table 1. At 48 h after transfection, the cells were incubated with 20 μM mitoxantrone for 1 h at 37°C. Mitoxantrone fluorescence in arbitrary units was determined by flow cytometry with a 635 nm red diode laser and 661 nm bandpass filter. Each column represents the mean ± SEM ($n = 3$). $^{**}p < 0.01$, significantly different from the NC siRNA-treated HEK293 cells co-transfected with myc-tagged rABCG2 cDNA (NC +). (b) Representative histogram plot and dot plot of HEK293 cells transfected with siRNAs [NC siRNA or rABCG2 siRNA-03 (03)] with (+) or without (–) myc-tagged rABCG2 cDNA, showing the mitoxantrone fluorescence vs. cell number and side scattered light (SSC), respectively. The gated cell population (solid line) identified the mitoxantrone-effluxing cells. The number shown is the proportion of total rABCG2-transfected cells contained in the gated cell population (mean ± SEM; $n = 3$).

exogenous rABCG2 protein was also completely suppressed at 24 h and 72 h after rABCG2 siRNA-03 transfection (Fig. 2), indicating that this siRNA remains effective at least from 24 h to 72 h. The sequence of rABCG2 siRNA-03 is 100% identical with the corresponding sequence of mouse ABCG2 (GenBank accession number NM011920). Therefore, this siRNA could be also effective for suppressing the function of mouse ABCG2.

The sequence locations of the effective rABCG2 siRNA-01, rABCG2 siRNA-03 and rABCG2 siRNA-04 (Table 1) were not limited to within 100-nucleotides downstream from the first ATG in contrast to the previous siRNA design (Elbashir *et al.* 2002). This result is in agreement with the recent report indicating that the major determinant of siRNA activity is the target sequence itself, rather than its location (Yoshinari *et al.* 2004). Recently, eight criteria for rational siRNA design for RNA interference were proposed (Reynolds *et al.* 2004). Indeed, the most effective rABCG2 siRNA (rABCG2 siRNA-03) satisfied as many as six of the criteria. For instance, this siRNA has moderate to low G/C content (30–52%), low internal stability of the sense 3′-end (at least three A/U bases at 15–19 nt) and a lack of internal repeats. Moreover, rABCG2 siRNA-03 has 'A' and 'U' at positions 19 and 10, respectively. It has been reported that these sequence-related criteria had a strong impact on improved selection of highly potent siRNAs (the increase in the probability of selecting siRNAs which induce more than 95% gene silencing was 7.2% and 12.8% for A19 and U10, respectively; Reynolds *et al.* 2004).

The present study has demonstrated that the delivery of siRNA suppresses rABCG2 mRNA and protein expression in TR-BBB13 cells (Figs 4a and 5), which are an *in vitro* BBB model expressing functional rABCG2 (Hori *et al.* 2004). There have been reports that the protein and function of targeted transporters were suppressed concomitantly with silencing of the corresponding genes (Wu *et al.* 2003; Nabokina *et al.* 2004; Said *et al.* 2004). Indeed, the endogenous rABCG2 protein level was suppressed in TR-BBB13 cells concomitantly with its gene silencing. rABCG2 siRNA-03 presumably suppresses transport activity of endogenous rABCG2 in TR-BBB13 cells by the reduction of rABCG2 protein level. The rABCG2 siRNA suppressed the induction of the rABCG2 mRNA level by 17β-estradiol to the same level as in untreated cells (Fig. 4a). This result suggests that this siRNA was efficiently delivered into TR-BBB13 cells and blocked the induced gene expression of rABCG2. Further study using labeled siRNA would be useful for distinguishing the transfection efficiency of siRNA from the efficacy of siRNA on endogenous rABCG2.

The rABCG2 mRNA level increased in TR-BBB13 cells following treatment with 100 nM 17β-estradiol (Fig. 4). Estrogen is thought to reach a maximum concentration of

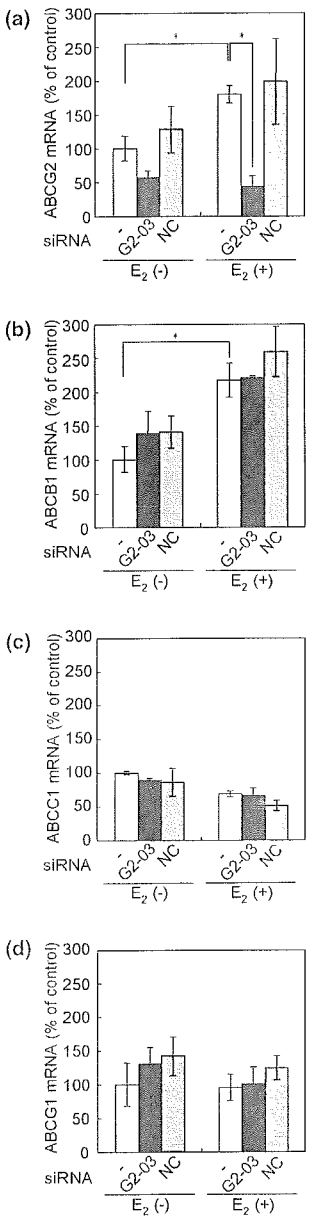

Fig. 4 Selective gene silencing of rABCG2 in TR-BBB13 cells by siRNA.TR-BBB13 cells were transfected with rABCG2 siRNA-03 (G2-03, ■) or non-specific control siRNA (NC, ▨), or untransfected (–, □). After 24 h transfection of siRNAs, the culture medium was changed to that with (+) or without (–) 17β-estradiol (E_2), and culture was continued for another 24 h. The ABCG2 (a), ABCB1 (b), ABCC1 (c), and ABCG1 (d) mRNA levels were determined by quantitative real-time PCR analysis. Each column represents the mean ± SEM ($n = 3$). Each mRNA level was normalized relative to the β-actin mRNA level. Each mRNA level is shown as percentage of the mean of the mRNA levels in TR-BBB13 cells treated with non-siRNA (–) and 17β-estradiol (E_2) (the leftmost column). $^*p < 0.05$, significant difference.

150 nM during the third trimester of pregnancy (Clarke *et al.* 2001). Under such conditions, there is possibility that brain-to-blood transport activity via ABCG2 would be induced.

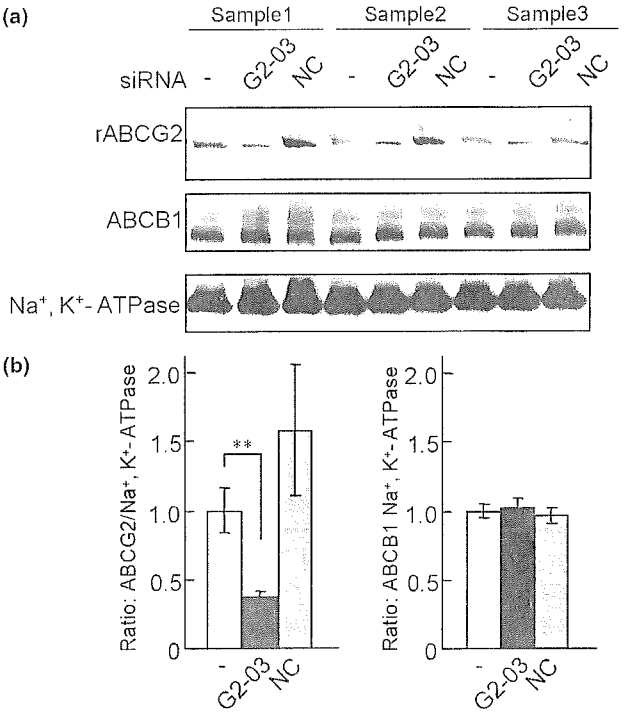

Fig. 5 Selective suppression of rABCG2 protein expression in TR-BBB13 cells by siRNA.TR-BBB13 cells were transfected with rABCG2 siRNA-03 (G2-03) or non-specific control siRNA (NC), or untransfected (–). After 36 h transfection of siRNAs, the cells were collected for western blot analysis using anti-ABCG2, anti-ABCB1 and anti-Na^+,K^+-ATPase antibodies.(a) Results from three independent western blot analyses (samples 1–3) are shown. (b) The ratio of ABCG2 (left panel) or ABCB1 (right panel) densities to Na^+,K^+-ATPase density. Each column represents the mean ± SEM ($n = 3$). $^{**}p < 0.01$, significantly different from untransfected cells (–).

17β-Estradiol also regulates the expression of ABCB1 and ABCC1 mRNAs in TR-BBB13 cells, suggesting that these ABC transporter-mediated transport systems may be affected by exposure to 17β-estradiol. Recently, it has been reported that the promoter region of human ABCG2 gene contains a novel and functional estrogen response element (ERE) which has 83.3% (10 aa/12 aa) homology with a classical consensus ERE (Ee *et al.* 2004). A search of the rat genome sequence revealed that the first intron of rABCG2 also has a sequence which shows 83.3% (10 aa/12 aa) homology with the classical consensus ERE. It has been reported that 17β-estradiol enhances the ABCG2 mRNA expression in estrogen receptor (ER)-positive human cancer cell lines (Ee *et al.* 2004), and that BCECs express multiple subtypes of ER-α (Stirone *et al.* 2003). Investigation of the sensitivity of the ERE-like sequence should provide a better understanding of the mechanism of rABCG2 induction by 17β-estradiol treatment.

Introduction of siRNA into TR-BBB13 cells would be a promising approach to clarify the specific role of each transporter at the BBB because the cells retain the *in vivo*

transport properties towards various compounds (Terasaki *et al.* 2003). The efficiency of a DNA vector-based transfection using cationic liposomes was less than 5% in TR-BBB13 cells (unpublished data). The present study suggests that oligonucleotide (siRNA)-based transfection is far more effective than DNA vector-based transfection in the case of TR-BBB13 cells. ABCG2 confers multidrug resistance upon cancer cells, so ABCG2 siRNA-induced RNA interference may also be useful for overcoming drug resistance.

The luminal localization of ABCG2 at the BBB has been clearly demonstrated in humans (Cooray *et al.* 2002) and rats (Hori *et al.* 2004). However, the functional contribution of ABCG2 at the BBB *in vivo* remains unclear (Allen and Schinkel 2002). Following rABCG2 siRNA-03 transfection into TR-BBB13 cells, the mRNA level of ABCG1, which has sequence homology with ABCG2, was unchanged (Fig. 4d), and those of ABCB1 and ABCC1, which can transport some ABCG2 substrates, were unaffected for at least 48 h after the siRNA transfection (Figs 4b.c). These data suggest that the silencing effect of the siRNA is specific for the ABCG2 gene in this *in vitro* BBB model. Because the rABCG2 siRNA selectively suppressed rABCG2 mRNA and protein, the siRNA study should allow us to clarify the contribution of the transporter to the BBB efflux transport. Indeed, it has recently been reported that siRNA designed to distinguish thiamine transporter subtypes induced subtype-specific gene silencing in Caco-2 cells, and that the functional contribution of the subtypes to thiamine uptake in the cells was clearly demonstrated by using the siRNA (Said *et al.* 2004). Such a sequence-specific silencing by siRNA may be a promising way to achieve a deeper understanding of the physiological and pharmacological roles of rABCG2 at the BBB. Regarding transporter gene knockdown at the BBB, the siRNA transfection into BCECs should be more specific than suppression by inhibitors, and easier to carry out as compared with the development of knockout mice. Moreover, the siRNA technique would be useful for silencing plural transporter genes because mixtures of siRNAs can be delivered.

In conclusion, the present study has demonstrated that delivery of siRNA into this *in vitro* BBB model specifically reduced endogenous rABCG2 protein level as well as its mRNA level. Application of the siRNA technique to BBB research should increase our understanding of ABCG2 role at the BBB.

Acknowledgements

We wish to thank Prof. M. Watanabe, Mr M. Tachikawa for helpful discussion and establishment of anti-ABCG2 antibody, and Messrs M. Fujiyoshi, N. Kimura for technical assistance. We would also like to thank Ms N. Funayama for secretarial assistance. This study was supported in part by a Grant-in-Aid for Scientific Research from Japan Society for the Promotion of Science, and a 21st Century COE Program Special Research Grant from the Ministry of Education Science, Sports and Culture. It was also supported in part by the Industrial Technology Research Grant Program from the New Energy and Industrial Technology Development Organization (NEDO) of Japan.

References

Allen J. D. and Schinkel A. H. (2002) Multidrug resistance and pharmacological protection mediated by the breast cancer resistance protein (BCRP/ABCG2). *Mol. Cancer Ther.* **1**, 427–434.

Allen J. D., van Loevezijn A., Lakhai J. M., van der Valk M., van Tellingen O., Reid G., Schellens J. H., Koomen G. J. and Schinkel A. H. (2002) Potent and specific inhibition of the breast cancer resistance protein multidrug transporter in vitro and in mouse intestine by a novel analogue of fumitremorgin C. *Mol. Cancer Ther.* **1**, 417–425.

Asaba H., Hosoya K., Takanaga H., Ohtsuki S., Tamura E., Takizawa T. and Terasaki T. (2000) Blood–brain barrier is involved in the efflux transport of a neuroactive steroid, dehydroepiandrosterone sulfate, via organic anion transporting polypeptide 2. *J. Neurochem.* **75**, 1907–1916.

de Bruin M., Miyake K., Litman T., Robey R. and Bates S. E. (1999) Reversal of resistance by GF120918 in cell lines expressing the ABC half-transporter, MXR. *Cancer Lett.* **146**, 117–126.

Clarke R., Leonessa F., Welch J. N. and Skaar T. C. (2001) Cellular and molecular pharmacology of antiestrogen action and resistance. *Pharmacol. Rev.* **53**, 25–71.

Cooray H. C., Blackmore C. G., Maskell L. and Barrand M. A. (2002) Localisation of breast cancer resistance protein in microvessel endothelium of human brain. *Neuroreport* **13**, 2059–2063.

Ee P. L., Kamalakaran S., Tonetti D., He X., Ross D. D. and Beck W. T. (2004) Identification of a novel estrogen response element in the breast cancer resistance protein (ABCG2) gene. *Cancer Res.* **64**, 1247–1251.

Elbashir S. M., Harborth J., Weber K. and Tuschl T. (2002) Analysis of gene function in somatic mammalian cells using small interfering RNAs. *Methods* **26**, 199–213.

Gao B., Stieger B., Noe B., Fritschy J. M. and Meier P. J. (1999) Localization of the organic anion transporting polypeptide 2 (Oatp2) in capillary endothelium and choroid plexus epithelium of rat brain. *J. Histochem. Cytochem.* **47**, 1255–1264.

Hannon G. J. (2002) RNA interference. *Nature* **418**, 244–251.

Hori S., Ohtsuki S., Tachikawa M., Kimura N., Kondo T., Watanabe M., Nakashima E. and Terasaki T. (2004) Functional expression of rat ABCG2 on the luminal side of brain capillaries and its enhancement by astrocyte-derived soluble factor(s). *J. Neurochem.* **90**, 526–536.

Hosoya K., Takashima T., Tetsuka K. *et al.* (2000a) mRNA expression and transport characterization of conditionally immortalized rat brain capillary endothelial cell lines; a new *in vitro* BBB model for drug targeting. *J. Drug Target.* **8**, 357–370.

Hosoya K., Tetsuka K., Nagase K. *et al.* (2000b) Conditionally immortalized brain capillary endothelial cell lines established from a transgenic mouse harboring temperature-sensitive simian virus 40 large T-antigen gene. *AAPS Pharmsci.* **2**, article 27. doi: 10.1208/ps020327 Available: http://www.aapspharmsci.org

Hosoya K., Ohtsuki S. and Terasaki T. (2002) Recent advances in the brain-to-blood efflux transport across the blood–brain barrier. *Int. J. Pharm.* **248**, 15–29.

Hyafil F., Vergely C., Du Vignaud P. and Grand-Perret T. (1993) *In vitro* and *in vivo* reversal of multidrug resistance by GF120918, an acridonecarboxamide derivative. *Cancer Res.* **53**, 4595–4602.

Mori S., Takanaga H., Ohtsuki S., Deguchi T., Kang Y. S., Hosoya K. and Terasaki T. (2003) Rat organic anion transporter 3 (rOAT3) is responsible for brain-to-blood efflux of homovanillic acid at the abluminal membrane of brain capillary endothelial cells. *J. Cereb. Blood Flow Metab.* **23**, 432–440.

Nabokina S. M., Ma T. Y. and Said H. M. (2004) Mechanism and regulation of folate uptake by the human pancreatic epithelial MIA PaCa-2 cells. *Am. J. Physiol. Cell Physiol.* **287**, C142–C148.

Rabindran S. K., Ross D. D., Doyle L. A., Yang W. and Greenberger L. M. (2000) Fumitremorgin C reverses multidrug resistance in cells transfected with the breast cancer resistance protein. *Cancer Res.* **60**, 47–50.

Reynolds A., Leake D., Boese Q., Scaringe S., Marshall W. S. and Khvorova A. (2004) Rational siRNA design for RNA interference. *Nat. Biotechnol.* **22**, 326–330.

Said H. M., Balamurugan K., Subramanian V. S. and Marchant J. S. (2004) Expression and functional contribution of hTHTR-2 in thiamine absorption in human intestine. *Am. J. Physiol. Gastrointest. Liver Physiol.* **286**, G491–G498.

Stirone C., Duckles S. P. and Krause D. N. (2003) Multiple forms of estrogen receptor-alpha in cerebral blood vessels: regulation by estrogen. *Am. J. Physiol. Endocrinol. Metab.* **284**, E184–E192.

Suzuki M., Suzuki H., Sugimoto Y. and Sugiyama Y. (2003) ABCG2 transports sulfated conjugates of steroids and xenobiotics. *J. Biol. Chem.* **278**, 22 644–22 649.

Terasaki T. and Hosoya K. (1999) The blood–brain barrier efflux transporters as a detoxifying system for the brain. *Adv. Drug Deliv. Rev.* **36**, 195–209.

Terasaki T., Ohtsuki S., Hori S., Takanaga H., Nakashima E. and Hosoya K. (2003) New approaches to *in vitro* models of blood–brain barrier drug transport. *Drug Discov. Today* **8**, 944–954.

Virgintino D., Robertson D., Errede M., Benagiano V., Girolamo F., Maiorano E., Roncali L. and Bertossi M. (2002) Expression of P-glycoprotein in human cerebral cortex microvessels. *J. Histochem. Cytochem.* **50**, 1671–1676.

Wu H., Hait W. N. and Yang J. M. (2003) Small interfering RNA-induced suppression of MDR1 (P-glycoprotein) restores sensitivity to multidrug-resistant cancer cells. *Cancer Res.* **63**, 1515–1519.

Yoshinari K., Miyagishi M. and Taira K. (2004) Effects on RNAi of the tight structure, sequence and position of the targeted region. *Nucl Acids Res.* **32**, 691–699.

Zelcer N., Reid G., Wielinga P., Kuil A., van der Heijden I., Schuetz J. D. and Borst P. (2003) Steroid and bile acid conjugates are substrates of human multidrug-resistance protein (MRP)4 (ATP-binding cassette C4). *Biochem. J.* **371**, 361–367.

Zhang Y., Boado R. J. and Pardridge W. M. (2003) *In vivo* knockdown of gene expression in brain cancer with intravenous RNAi in adult rats. *J. Gene Med.* **5**, 1039–1045.

OLIGONUCLEOTIDES 15:298–302 (2005)

Brief Communication

New RNAi Strategy for Selective Suppression of a Mutant Allele in Polyglutamine Disease

TAKAYUKI KUBODERA,[1,2*] TAKANORI YOKOTA,[1*] KINYA ISHIKAWA,[1] and HIDEHIRO MIZUSAWA[1,2]

ABSTRACT

In gene therapy of dominantly inherited diseases with small interfering RNA (siRNA), mutant allele-specific suppression may be necessary for diseases in which the defective gene normally has an important role. It is difficult, however, to design a mutant allele-specific siRNA for trinucleotide repeat diseases in which the difference of sequences is only repeat length. To overcome this problem, we use a new RNA interference (RNAi) strategy for selective suppression of mutant alleles. Both mutant and wild-type alleles are inhibited by the most effective siRNA, and wild-type protein is restored using the wild-type mRNA modified to be resistant to the siRNA. Here, we applied this method to spinocerebellar ataxia type 6 (SCA6). We discuss its feasibility and problems for future gene therapy.

INTRODUCTION

RNA INTERFERENCE (RNAi) is a powerful tool for posttranscriptional gene silencing. Small interfering RNA (siRNA) binds and cleaves the targeted RNA in a sequence-specific manner, thereby preventing translation of the encoded protein (Elbashir et al., 2001a). One possible therapeutic application of siRNA is the silencing of mutant genes that cause dominantly inherited diseases. We and others demonstrated that it is possible to design siRNA that selectively suppresses the expression of the mutant protein in amyotrophic lateral sclerosis (ALS), Alzheimer's disease, polyglutamine disease, and DYT1 dystonia (Gonzalez-Alegre et al., 2003; Miller et al., 2003, 2004; Li et al., 2004; Yokota et al., 2004). Recently, adeno-associated virus expressing siRNA injected into the cerebellum improved the polyglutamine-induced phenotype in a transgenic mouse model (Xia et al., 2004).

Although siRNA can discriminate even a single nucleotide alternation (Elbashir et al., 2001b), selectivity is not complete (Gonzalez-Alegre et al., 2003; Miller et al., 2003, 2004; Li et al., 2004; Yokota et al., 2004), and at a higher concentration of siRNA, the wild-type allele is more inhibited (Miller et al., 2004). In addition, the cleavage efficiency of the mutant allele is not necessarily excellent because selection of the mutant allele-specific siRNA has a restriction; that is, the siRNA target sequence should include the mismatch. In diseases caused by an expanded trinucleotide repeat, such as polyglutamine diseases, it is impossible to design siRNA that can recognize the expanded CAG repeat. In spinocerebellar ataxia type 3 (SCA3), a C/G polymorphism related to CAG repeat expansion has been used to design siRNA to discriminate the expanded allele (Miller et al., 2003; Li et al., 2004). We reported on siRNA with relative discrimination of the expanded allele of the SCA3 gene, which is possibly due to a

[1]Department of Neurology and Neurological Science, Graduate School, Tokyo Medical and Dental University, Bunkyo-ku, Tokyo 113-8519, Japan.

[2]21st Century COE Program on Brain Integration and Its Disorders, Tokyo Medical and Dental University, 1-5-45 Yushima, Bunkyo-ku, Tokyo 113-8519, Japan.

*These authors contributed equally to this work.

change in the RNA secondary structure (Li et al., 2004). In SCA6, however, the CAG repeat length in the mutant allele is within the normal range of other polyglutamine diseases, so that the secondary structure of RNA does not alter greatly even in the mutant. Here, we show a new alternate method for allele-specific suppression by siRNA. After suppressing both mutant and wild-type proteins by the most effective siRNA, wild-type protein is returned by coexpression of siRNA-resistant wild-type mRNA. This new strategy can be applied to any mutation.

MATERIALS AND METHODS

Plasmid construction and siRNA synthesis

Construction of expression plasmids of the α1A calcium channel gene (CACNA1A) was reported previously (Kubodera et al., 2003). The CACNA1A cDNA in the plasmid was truncated at the 3′-terminal region containing 13 (normal, pQ13C) or 28 (expanded, pQ28C) CAG repeats. Each construct corresponds to nucleotide positions 6727–7521 and 6727–7566 of the full-length CACNA1A cDNA. Modified pQ13C, in which CACNA1A cDNA is mutated not to be cleaved by siRNA7493 but translated to the same amino acids as those of pQ13C, was made by PCR amplification using pQ13C as a template (Fig. 1). The reverse primer included the modified mutations (light gray in Fig. 1), and the PCR fragment was subcloned into pcDNA3.1(+) (Invitrogen, San Diego, CA).

Selection of an siRNA target site was made according to the reported protocol (Reynolds et al., 2004). Sense and antisense strands of siRNA oligonucleotides (ODNs) were synthesized and prepared as described previously (Yokota et al., 2003). siRNA for an unrelated target, hepatitis C virus (HCV) gene, was used as a negative control.

Transfection and Western blotting

To see the effect of siRNA for CACNA1A mRNA, we cotransfected both siRNA and expression plasmids of CACNA1A to human emboryonic kidney 293T cells. Transfection was done with Lipofectamine Plus reagent (Invitrogen) according to the manufacturer's protocol.

For Western blotting at 24 hours posttransfection, cells were solubilized in lysis buffer (50 mM Tris-HCl, 150 mM NaCl, 1% Triton X-100), separated on a 10%–20% gradient of SDS-PAGE, immunoblotted with rabbit polyclonal antibody specific for the C-terminal portion of the α1A calcium channel protein (A6PRT-C) (Ishikawa et al., 1999), then made visible by enhanced chemiluminescence (ECL) (Amersham Bioscience, Buckinghamshire, England).

RESULTS

Using the synthetic siRNA (siRNA7493; 5′-ACAGCGAGAGUGACGAUGAdTdT-3′ in sense sequence), expressions of both wild-type (Q13C) and mutant (Q28C)

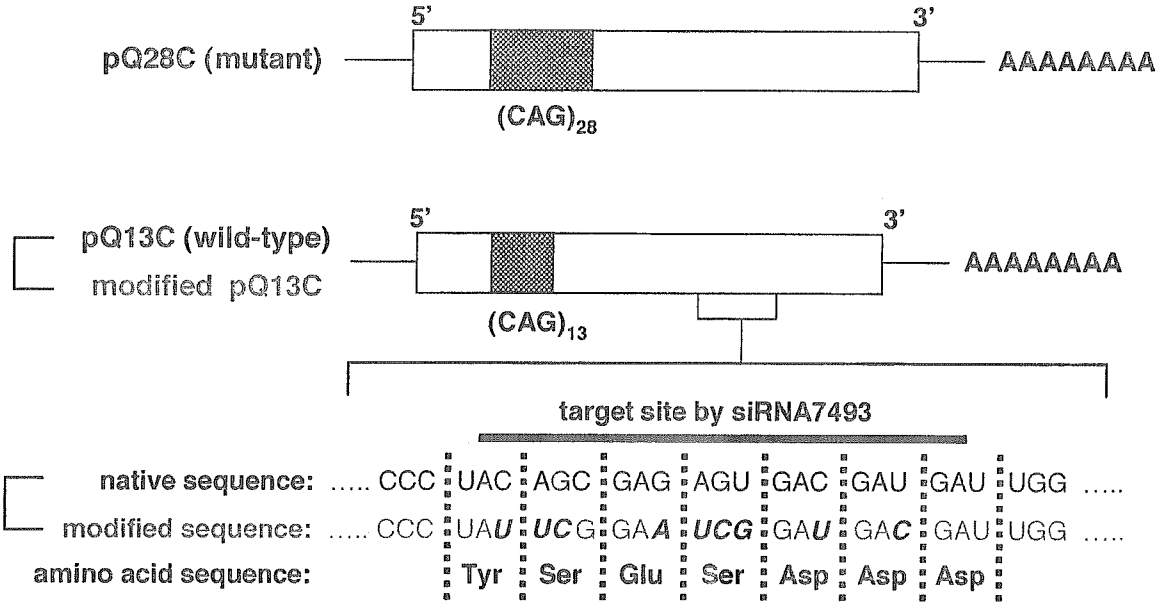

FIG. 1. Schema of mRNAs transcribed by expression plasmids of truncated CACNA1A. The RNA sequence around the target site of siRNA7493 is shown at bottom. The bold bar indicates the targeted sequence by siRNA7493. Characters in boldface italics are RNA nucleotides that are mutated from the wild-type. There is no change in amino acid sequences expressed by pQ13C or modified pQ13C.

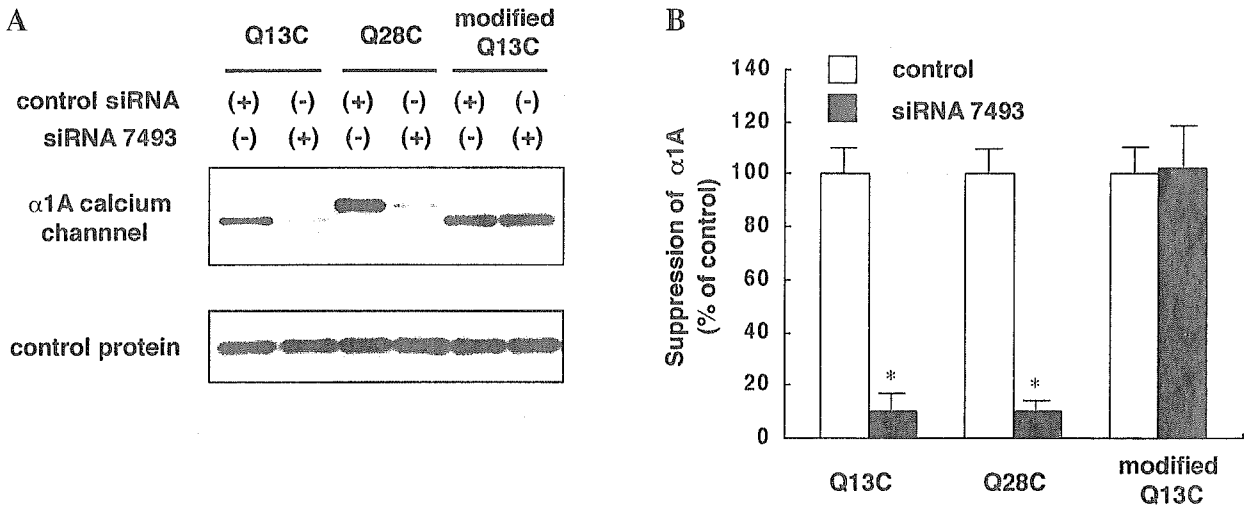

FIG. 2. Effect of siRNA7493 on expression of pQ13C, pQ28C, and modified pQ13C. (**A**) Western blot analysis of cells transfected with the indicated expression plasmids and control siRNA/siRNA7493 at 25 nM. The superoxide dismutase 1 (SOD1) protein staining was used as a loading control. (**B**) Quantitation of signal intensities. The suppression level of target protein was compared with transfection of control siRNA. siRNA7493 could markedly silence pQ13C and pQ28C but not modified pQ13C. Values are means ± SEM. *$p<0.001$ (Student's t-test).

α1A calcium channel proteins were markedly decreased by >90% on Western blot analysis (Fig. 2).

Because the siRNA7493 did not discriminate wild-type and mutant allele, we tried to restore the wild-type α1A calcium channel protein expressed by modified pQ13C, in which CACNA1A cDNA sequence is resistant to siRNA7493. We modified wild-type CACNA1A cDNA construct (modified pQ13C). The amino acid sequence encoded by modified pQ13C was the same as that of native pQ13C, but the nucleotide sequence targeted by siRNA was altered (Fig. 1). In fact, expression of modified pQ13C was not suppressed at all by siRNA7493 (Fig. 2).

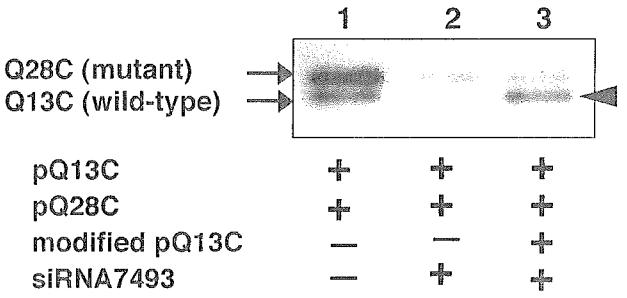

FIG. 3. Effect of siRNA7493 in cells cotransfected with pQ13C, pQ28C, or modified pQ13C (25 nM). Expressions of both pQ13C and pQ28C were markedly decreased by siRNA7493 (lane 2), but wild-type α1A calcium channel was restored to the same intensity level as that of lane 1 by expression of modified pQ13C (arrowhead) (lane 3). siRNA7493 (−) indicates no siRNA.

Next, we cotransfected modified pQ13C with pQ13C, pQ28C, and siRNA7493 to 293T cells. Modified pQ13C restored the expression of the wild-type α1A calcium channel that had been markedly inhibited by siRNA7493 (Fig. 3). Consequently, the mutant allele of CACNA1A was selectively silenced, whereas the wild-type protein was unchanged.

DISCUSSION

SCA6 is an autosomal dominant cerebellar ataxia characterized by late onset, pure cerebellar ataxia (Ishikawa et al., 1999). The causative gene for SCA6 has been identified as CAG repeat expansion in the α1A voltage-dependent calcium channel gene (Zhuchenko et al., 1997). The α1A subunit mediates Ca^{2+} influx across presynaptic and somatodendritic membranes, thereby triggering fast neurotransmitter release and other key neuronal responses. α1A-deficient mice develop ataxia and dystonia and die before 4 weeks of age (Jun et al., 1999), and the natural mutant mice of cacna1a, *leaner*, in which channel function is severely reduced, produce severe ataxia (Lorenzon et al., 1998). In gene therapy of SCA6 with siRNA, therefore, reduction of endogenous α1A calcium channel expression may produce an undesirable effect, and preservation of wild-type α1A calcium channel expression is necessary.

Our new method for allele-specific suppression by siRNA has the following advantages. (1) Any type of mutation can be applied by our method. (2) Only one set of the siRNA and wild-type protein-expressing vector in

our strategy works in many different mutants in a single gene; there are more than 100 mutations of superoxide dismutase 1 (SOD1) gene for familial ALS (*alsod1.iop.kcl.ac.uk/*) and presenilin 1 (PS1) gene for familial Alzheimer's disease (*www.molgen.ua.ac.be/ADMutations/*). (3) Greater than 90% suppression efficiency of mutant allele expression usually can be achieved using the recent prediction program of siRNA site (Reynolds et al., 2004) because the best siRNA site can be selected from the whole sequence of the target mRNA. In contrast, suppression efficiency of conventional siRNA should include the mutation, so that the target region is limited.

On the other hand, this method has the following important problems. (1) The expression level of the restored wild-type protein is difficult to control. If it is much greater than the endogenous level, it may produce an unexpected side effect. (2) Both siRNA and restored wild-type protein should be delivered to every cell, preferably by putting both expressing cassettes of short-hairpin RNA and siRNA-resistant wild-type cDNA into a single vector. To date, however, ODN is better than expression vectors for *in vivo* delivery of siRNA by systemic intravenous injection (Anton et al., 2002; Soutscheck et al., 2004). (3) There may be unknown differences of endogenous and exogenously expressed protein functions.

The efficacy of this strategy should be confirmed in an *in vivo* model, and the cited problems must be further addressed. Our new approach promotes the feasibility of using siRNA-based gene therapy for dominantly inherited diseases.

ACKNOWLEDGMENTS

We thank Toshinori Unno for his help. This work was supported by grants from the Ministry of Education, Science and Culture of Japan and from the Ministry of Health, Labor and Welfare of Japan.

REFERENCES

ANTON, P.M., LEONARD, M., THU-THAO, T.P., DOUGLAS, S.C., GREGORY, J.H., and MARK, K. (2002). RNA interference in adult mice. Nature **418,** 38–39.

ELBASHIR, S., HARBORTH, J., LENDECKEL, W., YALCIN, A., WEBER, K., and TUSCHL, T. (2001a). Duplexes of 21 nucleotide RNAs mediate RNA interference in cultured mammalian cells. Nature **411,** 494–498.

ELBASHIR, S.M., MARTINEZ, J., PATKANIOESKA, A., LENDECKEL, W., and TUSCHL, T. (2001b). Functional anatomy of siRNAs for mediating efficient RNAi in *Drosophila melanogaster* embryo lysate. EMBO J. **20,** 6877–6888.

GONZALEZ-ALEGRE, P., MILLER, V.M., DAVIDSON, B.L., and PAULSON, H.L. (2003). Toward therapy for DYT1 dystonia: Allele-specific silencing of mutant TorsinA. Ann. Neurol. **53,** 781–787.

ISHIKAWA, K., TUJIGASAKI, H., SAEGUSA, H., OHWADA, K., FUJITA, T., IWAMOTO, H., KOMATSUZAKI, Y., TORU, S., TORIYAMA, H., WATANABE, M., OHKOSHI, N., SHOJI, S., KANASAWA, I., TANABE, T., and MIZUSAWA, H. (1999). Abundant expression and cytoplasmic aggregations of α1A voltage-dependent calcium channel protein associated with neurodegeneration in spinocellebellar ataxia type 6. Hum. Mol. Genet. **8,** 1185–1193.

JUN, K., PIEDRAS-RENTERIA, E.S., SMITH, S.M., WHEELER, D.W., LEE, S.B., LEE, T.G., CHIN, H., ADAMS, M.E., SCHELLER, R.H., TSIEN, R.W., and SHIN, H.S. (1999). Ablation of P/Q-type $Ca^{(2+)}$ channel currents, altered synaptic transmission, and progressive ataxia in mice lacking the alpha(1A)-subunit. Proc. Natl. Acad. Sci. USA **96,** 15245–15250.

KUBODERA, T., YOKOTA, T., OHWADA, K., ISHIKAWA, K., MIURA, H., MATSUOKA, T., and MIZUSAWA, H. (2003). Proteolytic cleavage and cellular toxicity of the human α1A calcium channel in spinocerebellar ataxia type 6. Neurosci. Lett. **341,** 74–78.

LI, Y., YOKOTA, T., TAIRA, K., and MIZUSAWA, H. (2004). Sequence-dependent and independent inhibition specific for mutant ataxin-3 by small interfering RNA. Ann. Neurol. **56,** 124–129.

LORENZON, N.M., LUTZ, C.M., FRANKEL, W.N., and BEAM, K.G. (1998). Altered calcium channel currents in Purkinje cells of the neurological mutant mouse *leaner*. J. Neurosci. **18,** 4482–4489.

MILLER, V.M., GOUVION, C.M., DAVIDSON, B.L., and PAULSON, H.L. (2004). Targeting Alzheimer's disease genes with RNA interference: An efficient strategy for silencing mutant alleles. Nucleic Acids Res. **32,** 661–668.

MILLER, V.M., XIA, H., MARRS, G.L., GOUVION, C.M., LEE, G., DAVIDSON, B.L., and PAULSON, H.L. (2003). Allele-specific silencing of dominant disease genes. Proc. Natl. Acad. Sci. USA **100,** 7195–7200.

REYNOLDS, A., LEAKE, D., BOESE, Q., SCARINGE, S., MARSHALL, W.S., and KHVOROVA, A. (2004). Rational siRNA design for RNA interference. Nat. Biotechnol. **22,** 326–330.

SOUTSCHEK, J., AKINC, A., BRAMLAGE, B., CHARISSE, K., CONSTEIN, R., DONOGHUE, M., ELBASHIR, S., GEICK, A., HADWIGER, P., HARBORTH, J., JOHN, M., KESAVAN, V., LAVINE, G., PANDEY, R.K., RACIE, T., RAJEEV, K.G., ROHL, I., TOUDJARSKA, I., WANG, G., WUSCHKO, S., BUMCROT, D., KOTELIANSKY, V., LIMMER, S., MANOHARAN, M., and VORNLOCHER, H. (2004). Therapeutic silencing of an endogeneous gene by systemic administration of modified siRNAs. Nature **432,** 173–178.

XIA, H., MAO, Q., ELIASON, S.L., HARPER, S.Q., MARTINS, I., ORR, H., PAULSON, H.L., YANG, L., KOTIN, R.M., and DAVIDSON, B.L. (2004). RNAi suppresses polyglutamine-induced neurodegeneration in a model of spinocerebellar ataxia. Nat. Med. **10,** 816–820.

YOKOTA, T., MIYAGISHI, M., HINO, T., MATSUMURA,

R., ANDREA, T., URUSHITANI, M., RAO, R.V., TAKAHASHI, R., BREDESEN, D.E., TAIRA, K., and MIZUSAWA, H. (2004). siRNA-based inhibition of superoxide dismutase expression: Potential use in familial amyotrophic lateral sclerosis. Biochem. Biophys. Res. Commun. **314,** 283–291.

YOKOTA, T., SAKAMOTO, N., ENOMOTO, Y., TANABE, Y., MIYAGISHI, M., MAEKAWA, S., LI, Y., KUROSAKI, M., TAIRA, K., WATANABE, M., and MIZUSAWA, H. (2003). Inhibition of intracellular hepatitis C virus replication by synthetic and vector-derived small interfering RNAs. EMBO Rep. **4,** 602–608.

ZHUCHENKO, O., BAILEY, J., BONNEN, P., ASHIZAWA, T. STOCKTON, D.W., AMOS, C., DOBYNS, W.B., SUBRAMONY, S.H., ZOHGBI, H.Y., and LEE, C.H. (1997). Autosomal dominant cerebellar ataxia (SCA6) associated with small polyglutamine expansions in the alpha 1A-voltage-dependent calcium channel. Nat. Genet. **15,** 62–69.

Address reprint requests to:
Dr. Takanori Yokota
Department of Neurology and Neurological Science
Tokyo Medical and Dental University
1-5-45 Yushima
Bunkyo-ku
Tokyo 113-8519
Japan

E-mail: tak-yokota.nuro@tmd.ac.jp

Received April 21, 2005; accepted in revised form June 28, 2005.

Escape from the interferon response associated with RNA interference using vectors that encode long modified hairpin-RNA†

Hideo Akashi,‡[a] Makoto Miyagishi,‡*[ab] Takanori Yokota,[c] Tsunamasa Watanabe,[d] Taro Hino,[c] Kazutaka Nishina,[c] Michinori Kohara[d] and Kazunari Taira*[ab]

Received 18th July 2005, Accepted 12th October 2005
First published as an Advance Article on the web 7th November 2005
DOI: 10.1039/b510159j

In mammalian cells, siRNAs have been used to induce RNA interference (RNAi) in an attempt to prevent nonspecific effects (including the interferon (IFN) response) which are caused by long double-stranded RNAs (dsRNAs) of more than 30 bp. In this report, we describe a novel and simple strategy for avoiding activation of the IFN response by dsRNA. We show that modified hairpin-RNAs (mhRNAs) of more than 100 bp, with multiple specific point-mutations within the sense strand and transcribed from the U6 or $tRNA^{Val}$ promoters, can cause RNAi without inducing the IFN pathway genes. Moreover, we demonstrate that the 50-bp mhRNA vector could effectively suppress the replication of multiple hepatitis C viruses (the genomes of which differ slightly, thus the 21-bp siRNA vector failed to suppress one of them). Our findings should enhance the exploitation of RNAi in mammalian cells, especially in the field of RNAi therapy against pathogenic viruses.

Introduction

RNA interference (RNAi) is a post-transcriptional gene-silencing phenomenon that is triggered by double-stranded RNA (dsRNA). The initiator of RNAi is a 21- to 23-nucleotide (nt) dsRNA with a 2-nt 3′ overhang (siRNA), which is generated from long dsRNA by Dicer, a member of the RNase III family. The siRNA is incorporated into the multicomponent ribonucleoprotein complex (RISC) which cleaves mRNA that is complementary to the sequence of the siRNA.[1,2]

RNAi caused by long dsRNAs of 500 bp or so has been exploited in various species as a powerful genetic tool, since the technique is simple, and the suppressive effects on gene expression are both strong and specific. However, in mammalian cells, cytoplasmic dsRNAs of more than 30 bp induce nonspecific induction and/or suppression of the expression of many genes, which might result from the activation of dsRNA-dependent protein kinase (PKR) and 2′,5′-oligoadenylate synthetase (2′,5′-OAS), *via* a pathway known as the interferon (IFN) pathway.[3] Upon entry of dsRNA into cells, activation of PKR and 2′,5′-OAS results in the inhibition of translation and the nonspecific degradation of mRNA, respectively. Initially, the IFN response hampered the experimental application of RNAi to mammalian cells, except in the case of certain specific types of cell, such as early embryos and oocytes, until it was determined that siRNAs of 21 bp can circumvent the IFN response.[4]

General methods for preventing activation of components of the IFN system, including PKR and eukaryotic translation initiation factor 2 (eIF2α), have not been fully characterized, in spite of their obvious importance. In this study, we developed a simple but general strategy for prevention of the activation of the IFN system in mammalian cells. We show here that modified hairpin-RNAs (mhRNAs) of 50 bp or longer with multiple point mutations, which are transcribed from a U6 or tRNA promoter, can cause potent and specific gene silencing without the induction of IFN pathway genes in mammalian cells. Moreover, we show that the 50-bp mhRNA expression vector could effectively suppress the hepatitis C virus, whose genomes were mutated and could escape from RNAi caused by 21 bp siRNA expression vector.

Results

Nonspecific effects caused by dsRNA of longer than 30 bp in HeLa S3 cells

To quantitate the level of nonspecific effects (Fig. 1), we first examined an *in vitro* transcribed 50-bp dsRNA, which was targeted to a firefly gene for luciferase (luc). Various amounts of *in vitro* synthesized dsRNA were introduced into HeLa S3 cells with a luc expression plasmid and a *Renilla* luciferase (Rluc) expression plasmid (Fig. 1a). The *in vitro* transcribed dsRNA apparently suppressed the relative luc activity in a dose-dependent manner (Fig. 1a, left panel). However, it was

[a]*Department of Chemistry and Biotechnology, School of Engineering, The University of Tokyo, 7-3-1 Hongo, Bunkyo-ku, Tokyo, 113-8656, Japan. E-mail: makoto-m@chembio.t.u-tokyo.ac.jp; tiara@chembio.t.u-tokyo.ac.jp*
[b]*Gene Function Research Center, National Institute of Advanced Industrial Science and Technology (AIST), Central 4, 1-1-1 Higashi, Tsukuba Science City, 305-8562*
[c]*Department of Neurology and Neurological Science, Tokyo Medical and Dental University, 1-5-45 Yushima, Bunkyo-ku, Tokyo, 113-8519, Japan*
[d]*Department of Microbiology and Cell Biology and Cell Physiology, Tokyo Metropolitan Institute of Medical Science, 3-18-22 Honkomagome, Bunkyo-ku, Tokyo, 113-8613, Japan*
† Electronic supplementary information (ESI) available: Nucleotide sequences. See DOI: 10.1039/b510159j
‡ The first two authors contributed equally to this work.

